



Incorporating carbon dioxide into a stoichiometric producer–grazer model

Colleen M. Davies¹ · Hao Wang¹

Received: 3 October 2020 / Revised: 24 June 2021 / Accepted: 6 September 2021

© The Author(s), under exclusive licence to Springer-Verlag GmbH Germany, part of Springer Nature 2021

Abstract

Climate change models predict increases in atmospheric carbon dioxide concentration. As ecosystems equilibrate with the atmosphere, stimulation of photosynthesis is expected to occur. However, growth limitation due to soil nutrients may potentially limit sequestration of carbon. Additionally, changes in producer nutritional quality may cause a decline in grazer populations. Here we extend the WKL model to allow for consideration of the impacts of elevated atmospheric carbon dioxide concentration on producer–grazer dynamics. We do so by explicitly tracking the free carbon in the medium and allowing the producer’s growth rate to be limited by available carbon instead of light. This model is analyzed using primarily local bifurcation analysis. Overall, these analyses show that carbon sequestration due to increased atmospheric carbon dioxide can be limited by insufficient available phosphorus. Furthermore, increased atmospheric carbon dioxide will cause decreased stoichiometric quality of producers where available phosphorus is limiting.

Keywords Carbon dioxide · Stoichiometric producer–grazer model · Bifurcation analysis · Sequestration of carbon · Phosphorus · Photosynthesis · Photorespiration

Mathematics Subject Classification 92B05 · 34C23 · 34D20 · 37G15

1 Introduction

Since the Industrial Revolution, Earth’s atmosphere has been experiencing an unprecedented rate of increase in carbon dioxide (Pachauri et al. 2014). Climate change models have predicted that atmospheric concentrations of carbon dioxide may surpass 700

✉ Hao Wang
hao8@ualberta.ca

¹ Department of Mathematical and Statistical Sciences, University of Alberta, Edmonton, AB T6G 2R3, Canada

ppm by 2100 from the current ambient level of approximately 390 ppm (Pachauri et al. 2014). Such a substantial change will likely have far-reaching impacts on the environment and all life on earth. Changes in the global carbon cycle may also influence the global phosphorus and nitrogen cycles due to their coupling through biological interactions (Hessen et al. 2013). The main mechanisms by which ecosystems are directly impacted by increased atmospheric carbon dioxide concentration are changes in photosynthesis, transpiration and respiration (Drake et al. 1997). However, there are also indirect impacts.

According to Elser et al. (2010), the three possible scaling links between atmospheric concentration of carbon dioxide and producer stoichiometry are: stimulation of producer photosynthesis, potentially leading to increased carbon sequestration subject to soil resource constraints; increased plant root to shoot ratios and leaf area, impacting photosynthetic capacity and nutrient requirements; and reduction in Rubisco production due to increased efficiency, allowing for reallocation of nitrogen. The increased rate and efficiency of photosynthesis in C_3 plants occur due to changes in the light-independent reactions (Drake et al. 1997).

Photosynthesis is divided into two main components: the light-dependent reactions, and the light-independent reactions. The light-dependent reactions use solar energy and water to produce the energy compound ATP and the electron carrier NADPH. The light-independent reactions, also known as the Calvin Cycle, use these two products to fix carbon dioxide into glucose. In particular, in the carbon fixation step of the Calvin Cycle, the enzyme ribulose-1,5-bisphosphate carboxylase/oxygenase (Rubisco) catalyzes the carboxylation reaction, in which the carbon dioxide molecule combines with a five-carbon acceptor molecule, ribulose-1,5-bisphosphate (RubP). The resulting 6-carbon molecule then undergoes several other reactions to ultimately either make glucose or regenerate the RubP acceptor molecule (Stitt et al. 2010).

However, Rubisco can also catalyse the oxygenation of RubP, which begins the “photosynthetic carbon oxidation or photorespiratory pathway (PCO), which decreases the net efficiency of photosynthesis by 20–50%” (Drake et al. 1997). Carbon dioxide (CO_2) competitively inhibits the oxygenation reaction, causing an increase in both Rubisco- and RubP-limited net photosynthesis (Drake et al. 1997). This decrease in oxygenation along with the fact that Rubisco is not CO_2 -saturated at the current atmospheric concentration of CO_2 in some plants are thought to be the reasons that increased concentrations of atmospheric CO_2 have been shown to increase the rate of photosynthesis in C_3 plants, which have no mechanisms in place to reduce photorespiration (Ainsworth and Rogers 2007). According to Ainsworth and Rogers (2007), we know that at room temperature approximately 23% of fixed carbon is lost due to photorespiration, and that with all oxygenation reactions replaced with carboxylation reactions, uptake of carbon dioxide would be increased by around 53%.

The meta-analysis of terrestrial plants completed by Du et al. (2019) showed that elevated carbon dioxide stimulates photosynthesis, causing an increase in plant carbon (C) and carbon to nitrogen ratio (C:N), and a decrease in plant nitrogen (N), phosphorus (P), and nitrogen to phosphorus ratio (N:P). Thus elevated atmospheric carbon dioxide has a larger impact on levels of N than P, likely due to the fact that a large proportion (approximately 25%) of the nitrogen in a leaf is in Rubisco (Drake et al. 1997). Notably, the slight increase in C:P was not statistically significant, despite the relatively large

sample size (Du et al. 2019). An alternative explanation for the differences between nitrogen and phosphorus could consider the growth-rate hypothesis (Du et al. 2019): increased growth rate is related to the decrease in N:P because phosphorus-rich RNA is required by plant organs for rapid protein synthesis (Sterner and Elser 2002).

There is also evidence that increasing atmospheric carbon dioxide concentration increases the rate of photosynthesis in aquatic producers. Experimentally, Urabe et al. (2003) found that increased atmospheric concentration of carbon dioxide also increases the partial pressure of carbon dioxide in water, resulting in the stimulation of algal growth. The saturation level of algal abundance was higher in the increased CO₂ treatments, suggesting that growth of algae in the control was limited by carbon dioxide. Furthermore, there was a significantly lower final algal cellular quota (P:C) for the elevated carbon dioxide treatments compared to the control treatment.

The rate of exchange of carbon dioxide between water and the air above is directly proportional to the concentration gradient of carbon dioxide across the water's surface (Low-Decarie et al. 2014). The proportionality constant, which is known as the gas exchange transfer velocity, is hard to determine due to its relationship with wind speed, which differs globally and temporally (Wanninkhof 2007). Despite the direct relationship between the exchange rate of carbon dioxide and the concentration gradient of the gas across the boundary, water bodies are rarely equilibrated with the atmosphere (Low-Decarie et al. 2014; van de Waal et al. 2010). They can either be carbon sources, such as in many freshwater lakes, or sinks, as in many oceans (Low-Decarie et al. 2014).

Due to dissolved organic carbon from terrestrial ecosystems being mineralized by bacteria into CO₂, lakes are often carbon dioxide sources (van de Waal et al. 2010). In natural lakes, the partial pressure of CO₂ can vary over four orders of magnitude and is impacted by environmental perturbations (Urabe et al. 2003). If algae species have carbon concentration mechanisms (CCMs) that allow them to use dissolved bicarbonate ions (HCO₃⁻) in photosynthesis efficiently, increased partial pressure of carbon dioxide in their lake (pCO₂) would have a reduced impact on their growth, since in most lakes pCO₂ is much lower than the concentration of HCO₃⁻ (Low-Decarie et al. 2014; Urabe et al. 2003). However, CCMs appear to operate less efficiently under light or nutrient limitation (Urabe et al. 2003). Therefore, an increase in atmospheric carbon dioxide may have a larger impact in natural lakes where both nutrient and light are not sufficiently abundant (Urabe et al. 2003).

Whether a water body is a carbon dioxide source or sink is determined primarily by the amount of terrestrial carbon that enters the water (van de Waal et al. 2010). However, in their experiments, Urabe et al. (2003) found that when algal biomass reached saturated levels in the elevated carbon dioxide treatments, the carbon dioxide in the water decreased to levels not significantly different from the control treatment. Hence, the amount of algae in the water can also impact the concentration of dissolved carbon dioxide, since their uptake rate of carbon dioxide can exceed the diffusion rate from the atmosphere (Urabe et al. 2003). Additional factors that can determine carbon dioxide concentration in ocean surface waters include mixing, temperature, salinity, respiration, and calcification (Burkhardt and Riebesell 1997).

Although the major direct impacts on ecosystems of atmospheric carbon dioxide concentration are related to the producer at the base of the food chain, there are also indirect impacts on the grazer. Since herbivores tend to have more rigid, higher nutrient

requirements, their food can become less than optimal if the nutrient content of their food falls below their requirement (Sterner and Elser 2002). Hence, the decrease in algal P:C that may result from increased atmospheric carbon dioxide concentration can result in a decrease in growth of the grazer (Urabe et al. 2003). Additional experiments conducted by Urabe et al. (2003) confirmed that the decrease in grazer growth they observed was due to the decreased algal P:C, and not due to a direct impact of carbon dioxide on the grazer or to excessive food levels interfering with feeding activities.

Models such as the LKE and WKL models track the flow of carbon and phosphorus through a producer-grazer system (Loladze et al. 2000; Wang et al. 2008). However, these stoichiometric models assume that the system is open to carbon, given the prevalence in the atmosphere and relatively rapid dissolution of carbon dioxide into water. Thus, the intention of this paper is to expand the WKL model to explicitly incorporate atmospheric carbon dioxide concentration by adding a variable for free carbon in the medium, and by allowing the producer's growth to be limited by available carbon. A limiting case of the model will be analyzed mathematically and numerically, with the intention of addressing the potential impact of elevated atmospheric carbon dioxide concentration on the absolute and relative amounts of nutrient in the producer, and moreover, the impact of this change on the persistence of the grazer population.

2 The model

2.1 Model formulation

The WKL model is a stoichiometric producer-grazer model which includes carbon and phosphorus (Wang et al. 2008). The variables are x , the density of carbon in the producer; p , the density of phosphorus in the producer; y , the density of carbon in the grazer; and P , the density of phosphorus in the medium.

The WKL model is composed of four ordinary differential equations (Wang et al. 2008). The change in the density of carbon in the producer (dx/dt) is determined by producer growth limited by both nutrient (p/q) and light (K) availabilities, and by uptake by grazers. The change in producer phosphorus (dp/dt) is determined by phosphorus uptake by the producer, and phosphorus loss due to grazing and producer recycling. The change in the density of carbon in the grazer (dy/dt) is determined by grazer growth limited by food quantity and food quality, and by grazer death and respiration loss. Lastly, the change in free phosphorus in the system is determined by phosphorus uptake by the producer, and by phosphorus recycling from the producer, from the dead grazer, and from grazer feces.

The WKL model requires two main assumptions, originally from Loladze et al. (2000). The first is that “the total mass of phosphorus in the entire system is fixed”, i.e., the system is closed to phosphorus (Wang et al. 2008). This assumption allows for the four-dimensional system to be reduced to three dimensions. The second assumption is that the phosphorus to carbon ratio (P:C) in the producer (p/x) varies above a fixed minimum q ($p/x \geq q$), while the grazer maintains a constant P:C, θ (Wang et al. 2008). From this second assumption, we know the density of phosphorus in the grazer is given by θy .

The parameters are r , the producer intrinsic growth rate (day^{-1}); K , the producer light-dependent carrying capacity ($(\text{mg C})/\text{l}$); q , the minimal producer P:C ($(\text{mg P})/(\text{mg C})$); \hat{e} , the grazer maximal conversion rate; θ , the constant grazer P:C ($(\text{mg P})/(\text{mg C})$); \hat{d} , the grazer loss rate (day^{-1}); and d , the producer phosphorus loss rate (day^{-1}) (Wang et al. 2008). Due to the second law of thermodynamics, $\hat{e} < 1$, and in reality, $\theta \gg q$ (Wang et al. 2008). Therefore, we assume herein that $\theta > q$.

The model also uses two functions: $f(x)$, which is the rate at which the grazers ingest producer biomass, and $g(P)$, which is the per capita phosphorus uptake rate of the producers (Wang et al. 2008). If we assume $f(x)$ and $g(P)$ take the form of the Holling type II functional response, then we have

$$f(x) = \frac{cx}{a+x},$$

$$g(P) = \frac{\hat{c}P}{\hat{a}+P}.$$

For the WKL model, f and g are assumed to be bounded and smooth functions which satisfy $f(0) = 0$, $f'(x) > 0$ for $x \geq 0$, and $f''(x) \leq 0$ for $x \geq 0$ (Wang et al. 2008). For the Holling type II functional responses chosen here, let c be the maximal rate of ingestion of producer biomass by the grazers (day^{-1}); \hat{c} be the producer maximal phosphorus uptake rate ($(\text{mg P})/(\text{mg C})/\text{day}$); a be the grazer carbon half-saturation constant ($(\text{mg C})/\text{l}$); and \hat{a} be the producer phosphorus half-saturation constant ($(\text{mg P})/\text{l}$) (Wang et al. 2008).

The model developed here to investigate the impacts of elevated atmospheric concentration of CO_2 on a producer-grazer system is a modification of the WKL model. In addition to explicitly tracking free carbon in the medium, we replace the constant light-dependent carrying capacity K with a carbon-dependent carrying capacity ($h(C)$). As in the WKL model, all parameters are assumed to be positive.

Here C is the free carbon in the medium. The producer’s growth follows Liebig’s Law of the Minimum, where the growth rate is now either limited by the amount of phosphorus in the producer (p/q) or a carbon-dependent carrying capacity based on availability in the medium ($h(C)$). These two factors are assumed to be independently colimiting. Previously, data was fit for the algae *Chlamydomonas acidophila* to four different Monod-type models for phosphorus and carbon limitation, and dependent colimitation was rejected in favour of independent limitation between these two factors (Spijkerman et al. 2011). Rather than using a multiplicative form of independent limitation, as in Spijkerman et al. (2011), we use Liebig’s Law of the Minimum for simplicity of analysis. There is no strong evidence for classification of colimitation between light and carbon, and therefore we assume that there is sufficient light in the system so as to be non-limiting.

The equations are

$$\frac{dx}{dt} = \underbrace{rx \left(1 - \frac{x}{\min\{p/q, h(C)\}} \right)}_{\text{producer growth limited by nutrient \& carbon}} - \underbrace{f(x)y}_{\text{uptake by grazers}} - \underbrace{\rho(C)l_x x}_{\text{respiration}}, \tag{1}$$

$$\frac{dy}{dt} = \underbrace{\hat{e} \min \left\{ 1, \frac{p/x}{\theta} \right\} f(x)y}_{\text{grazer growth limited by food quality \& quantity}} - \underbrace{\hat{d}y}_{\text{grazer death}} - \underbrace{l_y y}_{\text{respiration}}, \quad (2)$$

$$\frac{dp}{dt} = \underbrace{g(P)x}_{\text{P uptake by producer}} - \underbrace{\frac{P}{x} f(x)y}_{\text{P loss due to grazing}} - \underbrace{dp}_{\text{P loss due to producer recycling}}, \quad (3)$$

$$\begin{aligned} \frac{dP}{dt} = & \underbrace{-g(P)x}_{\text{P uptake by producer}} + \underbrace{dp}_{\text{P recycling from producer}} + \underbrace{\theta \hat{d}y}_{\text{P recycling from dead grazer}} \\ & + \underbrace{\left(\frac{P}{x} - \hat{e} \min \left\{ \theta, \frac{P}{x} \right\} \right) f(x)y}_{\text{P recycling from grazer feces}} + \underbrace{\theta l_y y}_{\text{P recycling from grazer respiration}}, \quad (4) \end{aligned}$$

$$\begin{aligned} \frac{dC}{dt} = & \underbrace{\rho(C)l_x x}_{\text{producer respiration}} + \underbrace{l_y y}_{\text{grazer respiration}} - \underbrace{r x \left(1 - \frac{x}{\min\{p/q, h(C)\}} \right)}_{\text{C uptake by producer}} \\ & + \underbrace{\left(1 - \hat{e} \min \left\{ 1, \frac{p/x}{\theta} \right\} \right) f(x)y}_{\text{C recycling from grazer feces}} + \underbrace{\hat{d}y}_{\text{C recycling from dead grazer}} + \underbrace{\alpha(\beta - C)}_{\text{C exchange}}. \quad (5) \end{aligned}$$

In order to model free carbon in the system, terms separately representing respiration have been added to the equations. Now Eq. (1) includes a term for producer respiration, where the rate of respiration is given by $\rho(C)l_x$. Equation (2) also includes a term for loss of carbon due to grazer respiration, where the rate of respiration is given by l_y . Note that whereas in the WKL model \hat{d} included grazer death and respiration loss, now \hat{d} is only for loss due to grazer death. Due to the assumption of strict homeostasis for the grazers, a term for compensatory loss of phosphorus due to respiration is now incorporated in Eq. (4). Lastly Eq. (5), which is for the free carbon in the medium, includes producer respiration, grazer respiration, uptake by the producer via photosynthesis, recycling from grazing, and then degradation/decomposition of dead grazers which is assumed to be instantaneous.

Equation (5) also includes a term for C exchange with the environment outside the system: $\alpha(\beta - C)$. Here β is the carbon density in the external medium, which is assumed to be constant; that is, the system has no impact on the external source of carbon dioxide. Hence, the rate of exchange of carbon dioxide is proportional to the gradient across the boundary, as in the literature (Low-Decarie et al. 2014). The parameter α is the rate of exchange between the system and the external environment, also known as the transfer velocity (Wanninkhof 2007). A higher value of α means the system is more “open”. Note that for $\alpha = 0$, we have a system which is locally closed, which is a limiting case of this open system. As $\alpha \rightarrow \infty$, the system becomes entirely open, and there is an essentially unlimited amount of carbon, as in the WKL model (Wang et al. 2008).

As aforementioned, $h(C)$ is the carbon-dependent carrying capacity of the producer. This term captures the limitation of carbon fixation by insufficient available carbon

dioxide, since Rubisco is not saturated at the current atmospheric concentration in some plants (Ainsworth and Rogers 2007). In general, we assume that $h(C)$ is non-decreasing, and that $h(0) = 0$. A basic choice for $h(C)$ is a scalar multiple of C ($h(C) = \gamma C$), although $h(C)$ should likely plateau at a value of C at which Rubisco is saturated.

In addition to incorporating the fact that Rubisco is not carbon dioxide saturated at ambient atmospheric concentrations, this model also includes the reduction in photorespiration rate due to competitive inhibition of the oxygenation reaction in Equation (1): $\rho(C)l_x$. Here $\rho(C)$ is a monotonically decreasing function of C which allows for the reduction of photorespiration at higher carbon levels. We observe that $\rho(C)$ should not tend towards 0 as $C \rightarrow \infty$ since the total respiration term should also include mitochondrial/cellular respiration.

For much of the analysis completed here, we assume the system is closed to carbon, i.e., that $\alpha = 0$, and that $\rho(C) = 1$. In that case, we let T_P be the total phosphorus in the system, and T_C be the total carbon in the system, where $T_P = p + P + \theta y$, and $T_C = x + y + C$. Hence, we can write $P = T_P - p - \theta y$ and $C = T_C - x - y$. Using Eqs. (1)–(5), it can be shown that $dT_P/dt = 0 = dT_C/dt$. Thus, through the Law of Conservation of Mass, we can reduce the dimension of the system in this limiting, closed case ($\alpha = 0, \rho(C) = 1$):

$$\frac{dx}{dt} = rx \left(1 - \frac{x}{\min\{p/q, h(T_C - x - y)\}} \right) - f(x)y - l_x x, \tag{6}$$

$$\frac{dy}{dt} = \hat{e} \min \left\{ 1, \frac{p/x}{\theta} \right\} f(x)y - \hat{d}y - l_y y, \tag{7}$$

$$\frac{dp}{dt} = g(T_P - p - \theta y)x - \frac{p}{x} f(x)y - dp. \tag{8}$$

2.2 Parameters

The parameters originally present in the WKL model were set at the values given in Wang et al. 2008, with the exception of \hat{d} which was adapted due to the separate loss terms in the equation for grazer carbon.

In order to select the ranges for the total carbon inside the closed limiting system (T_C) as well as the fixed external carbon (β), the atmospheric carbon dioxide concentrations used in the experiments conducted by Urabe et al. (2003) as well as the predicted concentration from Pachauri et al. (2014) were converted to carbon concentrations with classical stoichiometry. Urabe et al. (2003) used 360 ppm for ambient atmospheric carbon dioxide, which is equivalent to 360 mg/l, and one of the two elevated values used was 1500 ppm, which is equivalent to 1500 mg/l. As aforementioned, climate change models have predicted that the atmospheric concentration of carbon dioxide may surpass 700 ppm by 2100 (Pachauri et al. 2014). The atmospheric carbon dioxide concentrations of 360 mg/l, 700 mg/l, and 1500 mg/l were converted to 98.2 (mg C)/l, 191.0 (mg C)/l, and 409.4 (mg C)/l respectively using a relative atomic mass of carbon equal to 12.0107 g/mol and 15.9994 g/mol for oxygen, which gives a total mass of carbon dioxide of 44.0095 g/mol (Petrucci et al. 2011).

Table 1 The parameter (P) values (V) used for simulations

P	Description	V
r	Intrinsic growth rate of the producer	0.93 day^{-1}
c	Maximal ingestion rate of the grazer	0.75 day^{-1}
\hat{c}	Maximal phosphorus uptake rate of the producer	$0.2 \text{ (mg P)/(mg C)/day}$
a	Half-saturation constant of the grazer	0.25 (mg C)/l
\hat{a}	Phosphorus half-saturation constant of the producer	0.008 (mg P)/l
\hat{e}	Maximal conversion rate of the grazer	0.74
d	Phosphorus loss rate of the producer	0.05 day^{-1}
θ	Constant P:C of the grazer	$0.04 \text{ (mg P)/(mg C)}$
q	Minimal possible P:C of the producer	$0.004 \text{ (mg P)/(mg C)}$
T_P	Total phosphorus in the system	$0.003\text{--}0.3 \text{ (mg P)/l}$
T_C	Total carbon in the system	$98.2\text{--}409.4 \text{ (mg C)/l}$
\hat{d}	Death rate of the grazer	0.055 day^{-1}
l_x	Respiration rate of the producer	0.183 day^{-1}
l_y	Respiration rate of the grazer	0.165 day^{-1}
γ	Scaling factor for C dependent carrying capacity	$0.005\text{--}0.4202$
η	Asymptote for PCO function	0.901639
ζ	Difference between max and asymptote for PCO	0.670890
ξ	Exponent for PCO function	$0.019552 \text{ l/(mg C)}$
α	Rate of C exchange between system and exterior	$0\text{--}1e6 \text{ day}^{-1}$
β	Constant exterior C concentration	$98.2\text{--}409.4 \text{ (mg C)/l}$

The carbon-dependent carrying capacity is given by $h(C) = \gamma C$. The range of the parameter γ was selected dependent on the range of values for T_P . In particular, we determined what the carbon threshold for x would be dependent on the values of T_P studied by dividing them by q . For $T_P = 0.003$, this threshold is 0.75; for $T_P = 0.030$, 7.5; and for $T_P = 0.300$, 75. Therefore, for carbon limitation to occur at ambient carbon at roughly the same density as phosphorus limitation, we require $\gamma = 0.00764$, 0.0764, and 0.764 for $T_P = 0.003$, 0.030, and 0.300 respectively. Hence, for our analysis, we considered $\gamma \in \{0.005, 0.00764, 0.04202, 0.0764, 0.4202\}$, in order to observe examples of both carbon and phosphorus limitation of producer growth.

The respiration parameters were selected by adapting those of Diehl (2007) to the system parameters selected by Wang et al. (2008). Diehl modelled a *Daphnia*-algae system with explicit respiration of the grazer and algae, as well as a grazer death rate (Diehl 2007). The values assigned were 0.1 day^{-1} for algal respiration, 0.09 day^{-1} for grazer respiration, and 0.03 day^{-1} for the grazer death rate (Diehl 2007). Hence, the total loss rate for the grazer used by Diehl (2007) is 0.12 day^{-1} , which is less than the value used for the WKL model (Wang et al. 2008), which is 0.22 day^{-1} . In order to match the rest of the parameters in the system, the values used by Diehl (2007) were rescaled by the same factor (approximately 1.83) such that the total loss rate matched that in the WKL model (Wang et al. 2008).

The net respiration of the producer can be modelled using (von Caemmerer and Quick 2000)

$$\text{Net respiration} = \frac{2\Gamma_* V_{cmax}}{C_c + K_c(1 + O/K_o)} + R_d,$$

where C_c is the CO_2 partial pressure at the reaction site (μbar); Γ_* is the CO_2 partial pressure at which the carboxylation rate is equal to half the oxygenation rate (μbar); V_{cmax} is the maximal carboxylation rate ($\mu\text{mol m}^{-2}\text{s}^{-1}$); K_c is the CO_2 Michaelis Menten constant (μbar); O is the O_2 partial pressure at the reaction site (mbar); K_o is the O_2 Michaelis Menten constant (mbar); and R_d is the cellular respiration in light not associated with the PCO pathway ($\mu\text{mol m}^{-2}\text{s}^{-1}$). Note that some of these parameters vary between autotroph species. Values were selected from von Caemmerer and Quick (2000).

This equation produces a respiration rate in $\mu\text{mol m}^{-2}\text{s}^{-1}$. In Equation (1), $\rho(C)$ is a dimensionless quantity. However, the above formula can be used to find approximate values of the net respiration rate which can be rescaled such that $\rho(C) = 1$ at ambient carbon dioxide concentration. These values can then be used to find appropriate parameters for a function of the form $\rho(C) = \eta + \zeta e^{-\xi C}$. This form was selected to reduce the number of parameters and the complexity of estimating these quantities.

For the parameter that quantifies the degree of openness of the system in the open model, α , using $\alpha = 0$ would produce a system which is closed to carbon. As $\alpha \rightarrow \infty$, the model (with $\rho(C) = 1$) tends towards the completely open WKL system with producer respiration included and assuming abundant light. Thus, α was selected to range from 0 to 1,000,000 to give a broad range in order to begin to consider the impact of α on the system.

3 Mathematical analysis

3.1 Invariant set

Similar to the WKL model (Wang et al. 2008), we have a theorem that shows that solutions which start in a biologically meaningful region remain there for all forward time for the limiting closed case of the model ($\alpha = 0$, $\rho(C) = 1$). The region has several constraints. Within the region, x , y and p are all positive. Note that we cannot observe negative densities, and therefore this condition is biologically meaningful. Additionally, the carbon density of the producer is bounded above by the maximum phosphorus- and carbon-dependent carrying capacities, which would occur if all phosphorus and carbon in the system is in the medium. Also, the amounts of phosphorus and carbon in the combined biomass pools should not exceed the total amounts in the system. The proof of this theorem also very closely follows that of the dissipativity theorem for the WKL model (Wang et al. 2008). The proof of Theorem 1 is in ‘‘Appendix A’’.

Theorem 1 For the limiting case (6)–(8), the set

$$\Omega = \{(x, y, p): 0 < x < \min\{T_P/q, h(T_C)\}, 0 < y, 0 < p, p + \theta y < T_P, x + y < T_C\}$$

is positively invariant.

3.2 Equilibria

Consider the limiting case where $\alpha = 0$ and $\rho(C) = 1$, producing Eqs. (6)–(8). Let $h(C) = \gamma C$. We consider two cases for f and g , dependent on if both f and g are Holling type I or Holling type II functional responses.

First, we assume $f(x) = cx, g(P) = \hat{c}P$ and $h(C) = \gamma C$, i.e., that f and g are Holling type I functional responses. The resulting system and equations for equilibria are in ‘‘Appendix B’’.

The trivial extinction equilibrium $E_0 = (0, 0, 0)$ is a possible solution of the system. We can also explicitly find the forms of grazer extinction equilibria. The grazer extinction equilibria always take the form $(\bar{x}, 0, \bar{p})$, where \bar{x} and \bar{p} are decided by what is limiting the producer and other parameter-based conditions. There may also be coexistence equilibria.

The resulting equilibria for Holling type I functional responses for the limiting case are summarized in the following theorem.

Theorem 2 The simplified case of the model (6)–(8) with Holling type I functional responses has the trivial extinction equilibrium $E_0 = (0, 0, 0)$ which always exists, up to two grazer extinction equilibria, and may have coexistence equilibria, where the grazer extinction equilibria depend on two quantities:

$$A := \frac{\hat{c}\gamma T_P(r - l_x)^2 + (\hat{c}T_P - \hat{c}q\gamma T_C - dq\gamma)r(r - l_x) - dqr^2}{\hat{c}qr(r - l_x)},$$

and

$$B := \frac{\hat{c}\gamma T_P(r - l_x)^2 + (\hat{c}T_P - \hat{c}q\gamma T_C - dq\gamma)r(r - l_x) - dqr^2}{(\hat{c}q\gamma T_C(r - l_x) + dq(r + \gamma r - \gamma l_x))(r + \gamma r - \gamma l_x)}.$$

The grazer extinction equilibria satisfy:

- (i) If $A \leq 0$ and $B < 0$, then there is one grazer extinction equilibrium, given by

$$E_P := \left(\frac{\hat{c}T_P(r - l_x) - dqr}{\hat{c}qr}, 0, \frac{\hat{c}T_P(r - l_x) - dqr}{\hat{c}(r - l_x)} \right);$$

- (ii) If $A > 0$ and $B \geq 0$, then there is one grazer extinction equilibrium, given by

$$E_C := \left(\frac{\gamma T_C(r - l_x)}{r + \gamma r - \gamma l_x}, 0, \frac{\hat{c}\gamma T_C T_P(r - l_x)}{\hat{c}\gamma T_C(r - l_x) + d(r + \gamma r - \gamma l_x)} \right);$$

- (iii) If $A < 0$ and $B > 0$, then there are two grazer extinction equilibria, E_P and E_C ;
- (iv) If $A = B = 0$, then there is one grazer extinction equilibrium, $E_P = E_C$;
- (v) If $A > 0$ and $B < 0$, then there are no grazer extinction equilibria.

Second, we assume $f(x) = cx/(a + x)$, $g(P) = \hat{c}P/(\hat{a} + P)$, and $h(C) = \gamma C$, i.e., that f and g are Holling type II functional responses. The necessary system and equations used to find the equilibria are in ‘‘Appendix C’’.

The trivial extinction equilibrium $E_0 = (0, 0, 0)$ is a possible solution of this system. We can explicitly find the forms of the grazer extinction equilibria, dependent upon what is limiting the producer and other parameter-based conditions. Additionally, there may be coexistence equilibria, which are complicated to compute.

The following theorem summarizes the resulting equilibria.

Theorem 3 *The simplified case of the model (6)–(8) with Holling type II functional responses has the trivial extinction equilibrium $E_0 = (0, 0, 0)$ which always exists, up to three grazer extinction equilibria, and may have coexistence equilibria, where the grazer extinction equilibria depend upon three quantities:*

$$\begin{aligned}
 A &= \frac{\hat{c}rT_P(r - l_x) - dqr^2(\hat{a} + T_P) - \gamma T_C(\hat{c}qr(r - l_x) - dq^2r^2) + \hat{c}\gamma T_P(r - l_x)^2 - dqr\gamma(\hat{a} + T_P)(r - l_x)}{\hat{c}qr(r - l_x) - dq^2r^2}, \\
 B &= \frac{\hat{c}\gamma T_C(r - l_x) + d(\hat{a} + T_P)(r + \gamma r - \gamma l_x) - 2dqr\gamma T_C}{2d(r + \gamma r - \gamma l_x)} \\
 &\quad + \frac{\sqrt{(\hat{c}\gamma T_C(r - l_x) + d(\hat{a} + T_P)(r + \gamma r - \gamma l_x))^2 - 4\hat{c}d\gamma T_C T_P(r - l_x)(r + \gamma r - \gamma l_x)}}{2d(r + \gamma r - \gamma l_x)}, \\
 C &= \frac{\hat{c}\gamma T_C(r - l_x) + d(\hat{a} + T_P)(r + \gamma r - \gamma l_x) - 2dqr\gamma T_C}{2d(r + \gamma r - \gamma l_x)} \\
 &\quad - \frac{\sqrt{(\hat{c}\gamma T_C(r - l_x) + d(\hat{a} + T_P)(r + \gamma r - \gamma l_x))^2 - 4\hat{c}d\gamma T_C T_P(r - l_x)(r + \gamma r - \gamma l_x)}}{2d(r + \gamma r - \gamma l_x)}.
 \end{aligned}$$

The grazer extinction equilibria satisfy:

- (i) If $A \leq 0$, $B < 0$, and $C < 0$, then there is one grazer extinction equilibrium, given by

$$E_P = \left(\frac{\hat{c}T_P(r - l_x)^2 - dqr(\hat{a} + T_P)(r - l_x)}{\hat{c}qr(r - l_x) - dq^2r^2}, 0, \frac{\hat{c}T_P(r - l_x) - dqr(\hat{a} + T_P)}{\hat{c}(r - l_x) - dqr} \right);$$

- (ii) If $A > 0$, $B \geq 0$, and $C < 0$, then there is one grazer extinction equilibrium, given by $E_{C+} = (\bar{x}, 0, \bar{p}_+)$, where

$$\begin{aligned}
 \bar{x} &= \frac{\gamma T_C(r - l_x)}{r + \gamma r - \gamma l_x}, \\
 \bar{p}_+ &= \frac{\hat{c}\gamma T_C(r - l_x) + d(\hat{a} + T_P)(r + \gamma r - \gamma l_x)}{2d(r + \gamma r - \gamma l_x)} \\
 &\quad + \frac{\sqrt{(\hat{c}\gamma T_C(r - l_x) + d(\hat{a} + T_P)(r + \gamma r - \gamma l_x))^2 - 4\hat{c}d\gamma T_C T_P(r - l_x)(r + \gamma r - \gamma l_x)}}{2d(r + \gamma r - \gamma l_x)};
 \end{aligned}$$

(iii) If $A > 0$, $B < 0$, and $C \geq 0$, then there is one grazer extinction equilibrium, given by $E_{C-} = (\bar{x}, 0, \bar{p}_-)$, where

$$\begin{aligned} \bar{x} &= \frac{\gamma T_C(r - l_x)}{r + \gamma r - \gamma l_x}, \\ \bar{p}_- &= \frac{\hat{c}\gamma T_C(r - l_x) + d(\hat{a} + T_P)(r + \gamma r - \gamma l_x)}{2d(r + \gamma r - \gamma l_x)} \\ &\quad - \frac{\sqrt{(\hat{c}\gamma T_C(r - l_x) + d(\hat{a} + T_P)(r + \gamma r - \gamma l_x))^2 - 4\hat{c}d\gamma T_C T_P(r - l_x)(r + \gamma r - \gamma l_x)}}{2d(r + \gamma r - \gamma l_x)}; \end{aligned}$$

- (iv) If $A \leq 0$, $B \geq 0$, and $C < 0$, then there are two grazer extinction equilibria, E_P and E_{C+} ;
- (v) If $A \leq 0$, $B < 0$, and $C \geq 0$, then there are two grazer extinction equilibria, E_P and E_{C-} ;
- (vi) If $A > 0$, $B \geq 0$, and $C \geq 0$, then there are two grazer extinction equilibria, E_{C+} and E_{C-} ;
- (vii) If $A \leq 0$, $B \geq 0$, and $C \geq 0$, then there are three grazer extinction equilibria, E_P , E_{C+} , and E_{C-} ;
- (viii) If $A > 0$, $B < 0$, and $C < 0$, then there are no grazer extinction equilibria.

Note that the equilibria in the above theorem are not necessarily unique.

3.3 Stability

For the trivial extinction steady state, we have a theorem with a sufficient condition for stability in the limiting case of the model ($\alpha = 0$, $\rho(C) = 1$). This is very similar to a theorem proven for the WKL model (Davies and Wang 2020; Wang et al. 2008), and the proof follows similarly. Note that this theorem holds for the general forms of f , g , and h . The proof of Theorem 4 is in ‘‘Appendix D’’.

Theorem 4 *The extinction steady state $E_0 = (0, 0, 0)$ for (6)–(8) is globally asymptotically stable if $d > mg(T_P)$, where $m = \min\{x(0)/p(0), [1 + (d - l_x)/r]/q\}$.*

We can also investigate the stability of the grazer extinction equilibria for $\alpha = 0$ and $\rho(C) = 1$. We have

$$\begin{aligned} \frac{dx}{dt} &= xF(x, y, p), \\ \frac{dy}{dt} &= yG(x, y, p), \\ \frac{dp}{dt} &= H(x, y, p). \end{aligned}$$

The Jacobian matrix is

$$A = \begin{bmatrix} F + xF_x & xF_y & xF_p \\ yG_x & G + yG_y & yG_p \\ H_x & H_y & H_p \end{bmatrix}.$$

Once again, we consider Eqs. (6)–(8) where f and g are both Holling type I functional responses, then when both are Holling type II functional responses. Throughout, we assume $h(C) = \gamma C$.

Regardless of what forms f and g take, we consider four cases:

1. Producer is nutrient limited & grazer is quality (nutrient) limited at equilibrium.
2. Producer is nutrient limited & grazer is quantity (carbon) limited at equilibrium.
3. Producer is carbon limited & grazer is quality (nutrient) limited at equilibrium.
4. Producer is carbon limited & grazer is quantity (carbon) limited at equilibrium.

There are different Jacobian matrices dependent upon the limiting factors. We determine the entries based on what is limiting, then substitute the equilibria found in Sect. 3.2. From the Jacobian matrix, computation of the eigenvalues can be used to determine conditions for stability.

First, we use $f(x) = cx$, $g(P) = \hat{c}P$, and $h(C) = \gamma C$, i.e., f , g , and h are all Holling type I. All of the necessary partial derivatives and sums/products required, as well as the resulting Jacobian matrices and analysis of the eigenvalues are in “Appendix E”.

For the cases in which the producer’s growth is limited by nutrient, finding the eigenvalues is not particularly illuminating. However, from the explicit form of the eigenvalues, we do observe that stability does not depend upon T_C or γ when the grazer is quality limited (Case 1). Given that these factors pertain to carbon limitation, and thus do not appear in the equations in this case due to the minimum term, this result is not unexpected. When the grazer is quality limited (Case 2), stability does not depend on T_C , γ , or θ , because these parameters do not appear in the equations for the case where nutrient and quantity are limiting due to the minimum functions.

The stability results for Cases 3 and 4 using Holling type I functional responses are summarized in the following theorem. The proof is in “Appendix E”.

Theorem 5 *For the limiting case of the model (6)–(8) with Holling type I functional responses, the following stability results hold for the carbon-limited grazer extinction equilibrium $E_C = (\bar{x}, 0, \bar{p})$ from Theorem 2.*

- (i) *If $\bar{p} < \theta\bar{x}$, then the equilibrium is a stable node for either $r + \gamma r - \gamma l_x < 0$ or $r - l_x > 0$, and*

$$\frac{c\hat{c}\hat{e}\gamma T_C T_P (r - l_x)}{\hat{c}\gamma\theta T_C (r - l_x) + d\theta(r + \gamma r - \gamma l_x)} < \hat{d} + l_y,$$

and otherwise it is either a saddle with a one- or two-dimensional unstable manifold, or an unstable node.

- (ii) If $\bar{p} > \theta\bar{x}$, then the equilibrium is a stable node for either $r + \gamma r - \gamma l_x < 0$ or $r - l_x > 0$, and

$$\frac{c\hat{e}\gamma T_C(r - l_x)}{r + \gamma r - \gamma l_x} < \hat{d} + l_y,$$

and otherwise it is a saddle with a one- or two-dimensional unstable manifold.

Note that for Cases 3 and 4 we require either $r - l_x > 0$ and $r + \gamma r - \gamma l_x > 0$, or $r - l_x < 0$ and $r + \gamma r - \gamma l_x < 0$ for the equilibrium to be biologically feasible (see ‘‘Appendix B’’). Hence, the only biologically feasible classifications for the equilibrium in these cases are either a stable node or a saddle with a two-dimensional stable manifold and a one-dimensional unstable manifold.

Next, we let $f(x) = cx/(a + x)$, $g(P) = \hat{c}P/(\hat{a} + P)$, and $h(C) = \gamma C$, i.e., we let f and g be Holling type II. Again, there are different Jacobian matrices dependent upon the limiting factors. We determine the entries based on what is limiting, then substitute the equilibria found in Sect. 3.2. Eigenvalues are then computed and analyzed to determine conditions for stability of the equilibria. All of the necessary computations, eigenvalues, and analysis are in ‘‘Appendix F’’.

Once again, for the cases in which the producer is nutrient limited, the eigenvalues do not yield clear stability conditions. However, the same parameters that did not appear in the eigenvalues for the corresponding Holling type I cases also do not appear in these eigenvalues. That is, for the case where the grazer is quality limited (Case 1), stability does not depend on T_C or γ ; for the case where the grazer is quantity limited (Case 2), stability does not depend on T_C , γ , or θ .

The stability results for Cases 3 and 4 using Holling type II functional responses are summarized in the following theorem. The proof is in ‘‘Appendix F’’.

Theorem 6 *For the limiting case of the model (6)–(8) with Holling type II functional responses, the following stability results hold for the carbon-limited grazer extinction equilibria from Theorem 3, E_{C+} and E_{C-} , both of the form $(\bar{x}, 0, \bar{p})$.*

- (i) If $\bar{p} < \theta\bar{x}$, then the equilibrium is a stable node for either $r + \gamma r - \gamma l_x < 0$ or $r - l_x > 0$, and

$$\frac{c\hat{e}(r + \gamma r - \gamma l_x)\bar{p}}{a\theta(r + \gamma r - \gamma l_x) + \gamma\theta T_C(r - l_x)} < \hat{d} + l_y,$$

and otherwise it is either a saddle with a one- or two-dimensional unstable manifold, or an unstable node.

- (ii) If $\bar{p} > \theta\bar{x}$, then the equilibrium is a stable node for either $r + \gamma r - \gamma l_x < 0$ or $r - l_x > 0$, and

$$\frac{c\hat{e}\gamma T_C(r - l_x)}{a(r + \gamma r - \gamma l_x) + \gamma T_C(r - l_x)} < \hat{d} + l_y,$$

and otherwise it is either a saddle with a one- or two-dimensional unstable manifold, or an unstable node.

Note that biological feasibility of the equilibria requires $r - l_x$ and $r + \gamma r - \gamma l_x$ to have the same sign (see “Appendix C”). Hence, realistically, we would expect to only observe a stable node or a saddle with a two-dimensional stable manifold and a one-dimensional unstable manifold.

4 Numerical dynamics and their implications

4.1 Numerical simulations

For all numerical simulations, we used Holling type II functional responses for f and g ; that is, $f(x) = cx/(a + x)$, $g(P) = \hat{c}P/(\hat{a} + P)$, and $h(C) = \gamma C$. To study the impacts of different parameters and functions on the observed dynamics, simulations were run using Matlab’s ode23s, using a time span of $[0, 200]$. We simulated all combinations of $T_C \in \{98.2, 191.0, 409.4\}$, $T_P \in \{0.003, 0.030, 0.300\}$, $\gamma \in \{0.005, 0.00764, 0.0764\}$, and $\alpha \in \{0, 1e - 6, 1e - 3, 1e0, 1e3, 1e6\}$. We also used two different forms for $\rho(C)$: $\rho(C) = \eta + \zeta e^{-\xi C}$, and $\rho(C) = 1$, where the former was only used with $\alpha = 0$. Recall that our limiting, simplified case (6)–(8) uses $\alpha = 0$ and $\rho(C) = 1$. Initial conditions differed between parameter combinations dependent upon the value of T_P . For α nonzero, we used $C(0) = \beta - x(0) - y(0)$ for $\beta = T_C$.

The resulting dynamics were plotted and compared, with one example comparison in Fig. 1. The other plots are not shown here. We also individually graphed what was limiting the growth of the producer and grazer, as well as the producer P:C. All other parameters were held constant at the values given in Table 1.

To compare to the WKL model, we also simulated a version of the model with $\alpha = 0$, $\rho(C) = 1$, and without carbon limitation of the producer’s growth rate (i.e., assuming $h(C)$ is sufficiently high relative to T_P such that carbon limitation will never occur). Regardless of T_P , this case tended towards the grazer extinction equilibrium, $(\bar{x}, 0, \bar{p})$, because without light limitation, the producers become poor quality food for the grazers, as discussed in Wang et al. (2008). The value of \bar{x} and \bar{p} did vary depending upon T_P . Both \bar{x} and \bar{p} roughly scaled with T_P , increasing approximately tenfold when T_P was multiplied by ten.

Some problems were encountered for a couple of the parameter combinations. More specifically, for $\gamma = 0.0764$, $T_C = 98.2$ or 191.0 , and $T_P = 0.300$, several of the simulations failed. Despite the usage of ode23s, these cases produced results with negative species densities before $t = 200$. This behaviour was also observed for some simulations during bifurcation analysis.

Regardless of α or $\rho(C)$, we tend to observe grazer extinction when one of the limiting parameters (T_P or T_C) is very low. Assuming the other limiting parameter remains non-limiting, then as the limiting parameter increases, the system switches to coexistence at an equilibrium, then coexistence in oscillations, then an additional coexistence equilibrium, and then it returns to the grazer extinction equilibrium. This is further explored for the limiting case of $\alpha = 0$ and $\rho(C) = 1$ in the following bifurcation analysis (Sect. 4.2).

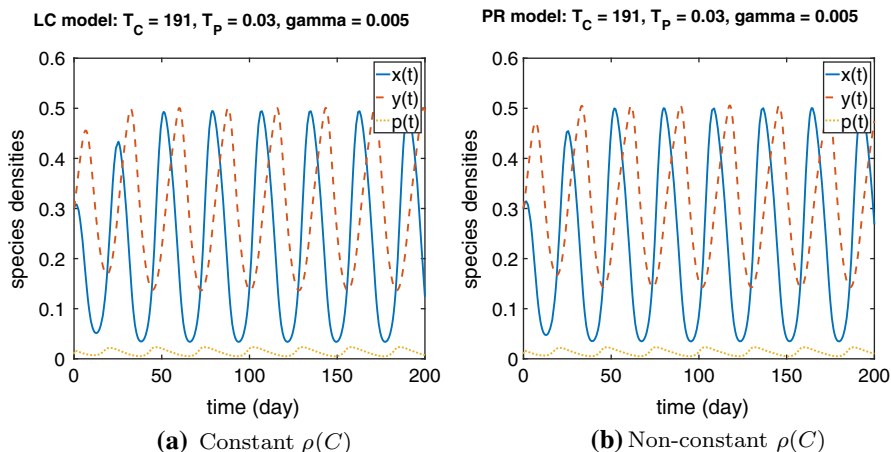


Fig. 1 Dynamics for $\gamma = 0.005, T_C = 409.4, T_P = 0.300$. We note the difference in $x(200)$, indicative of a slightly different period, as well as the slightly higher crests for x for non-constant $\rho(C)$

For all cases, minor differences between the asymptotic states given different α or $\rho(C)$ were observed. In general, these differences are not perceptible from the graphs. However, examination of the end values of the simulations showed that changing $\rho(C)$ (with $\alpha = 0$) was more impactful. For non-constant $\rho(C)$ and higher total carbon levels, the system demonstrated different periods of oscillations, as well as different maximum or minimum values, relative to $\rho(C) = 1$. An example of this minor difference is shown in Fig. 1.

4.2 One parameter bifurcation analysis

In order to compare and contrast the impacts on dynamics of the parameters that determine limitation of the producer, bifurcation analysis was performed for T_C and T_P for the limiting closed case of the model ($\alpha = 0, \rho(C) = 1$), shown in Eqs. (6)–(8), using Matcont (Dhooge et al. 2008). Multiple diagrams were generated for each parameter, varying the other parameter as well as γ to get as broad an idea of the impact of each parameter as reasonably possible. For T_P , we initially made bifurcation diagrams for all combinations of $T_C \in \{98.2, 191.0, 409.4\}$ and $\gamma \in \{0.005, 0.00764, 0.04202, 0.0764, 0.4202\}$. For T_C , we initially made bifurcation diagrams for all combinations of $T_P \in \{0.003, 0.030, 0.300\}$, and $\gamma \in \{0.005, 0.00764, 0.04202, 0.0764, 0.4202\}$. After beginning the two parameter bifurcation analysis we created several additional diagrams, all for $\gamma = 0.005$. For the total phosphorus diagrams, we also examined $T_C \in \{50, 75, 90, 150, 270, 275, 500\}$; for the total carbon diagrams, we added $T_P \in \{0.007, 0.010, 0.018, 0.022325, 0.025\}$.

For all one parameter diagrams, a solid blue curve represents a stable equilibrium point, a magenta dashed curve is an unstable equilibrium point, and a red dotted curve represents the minimum/maximum of a stable limit cycle.

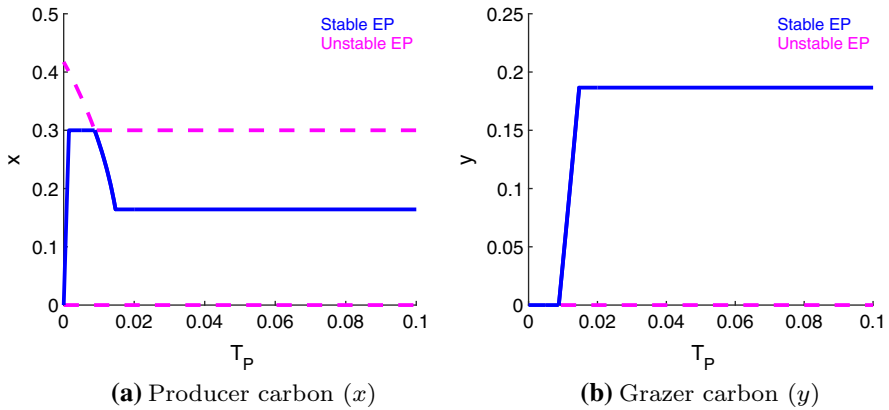


Fig. 2 T_P bifurcation diagrams: $T_C = 75$, $\gamma = 0.005$. x is on the left and y is on the right. There is a transcritical bifurcation at $T_P = 0.008779$. For $T_P < 0.008779$, a grazer extinction equilibrium is stable and for $T_P > 0.008779$, a coexistence equilibrium is stable

4.2.1 Total system phosphorus

For total system phosphorus, T_P , we observed five different types of diagram pairs.

The first type of diagram pair occurred for a couple of parameter combinations, with very low γ and less than ambient carbon ($\gamma = 0.005$, $T_C \in \{50, 75\}$). The only bifurcation is a transcritical bifurcation. For values of T_P less than the bifurcation value, a grazer extinction equilibrium is stable; for values greater than the bifurcation value, a coexistence equilibrium is stable. The equilibrium value plateaus as total phosphorus increases when the grazer switches from quality (phosphorus) limitation to quantity (carbon) limitation. An example of this behaviour is shown in Fig. 2. We observe that for these combinations, we have $\gamma * T_C = 0.25$ and 0.375 . For the higher value of T_C (and thus $\gamma * T_C$), the transcritical bifurcation occurs at a higher value of T_P .

The second type of diagram pair occurred for two combinations: very low γ and at or close to ambient carbon ($\gamma = 0.005$, $T_C \in \{90, 98.2\}$). Initially, a grazer extinction equilibrium is stable. Then, after a transcritical bifurcation, the grazer extinction equilibrium becomes unstable and a coexistence equilibrium is stable. This continues until a saddle-node bifurcation, at which point the coexistence equilibrium becomes unstable. At a very slightly higher value of T_P , we then have another saddle-node bifurcation, after which a different coexistence equilibrium becomes stable. Sample diagrams are shown in Fig. 3. For these combinations, $\gamma * T_C = 0.45$ and 0.491 . Similar to the previous type, a higher value of T_C (and thus $\gamma * T_C$) correlated to higher bifurcation values.

The third type of diagram pair occurred for two combinations: low γ and ambient carbon ($\gamma = 0.00764$, $T_C = 98.2$), and very low γ and intermediate carbon ($\gamma = 0.005$, $T_C = 191.0$). For sufficiently low T_P , a grazer extinction equilibrium is stable. Then, after a transcritical bifurcation, a coexistence equilibrium is stable, until a saddle-node bifurcation. There is an additional saddle-node bifurcation between the other two bifurcations, at which point there is a second coexistence equilibrium which

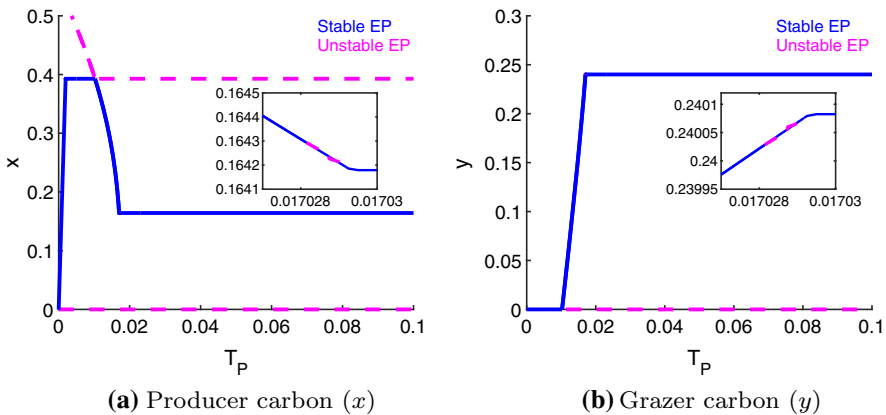


Fig. 3 T_P bifurcation diagrams: $T_C = 98.2$, $\gamma = 0.005$. x is on the left and y is on the right. There is a transcritical bifurcation at $T_P = 0.01024$, a saddle-node bifurcation at $T_P = 0.017028$, and another saddle-node bifurcation at $T_P = 0.017029$ (see embedded plots). For $T_P < 0.01024$, a grazer extinction equilibrium is stable; for $0.01024 < T_P < 0.017028$, a coexistence equilibrium is feasible and stable; and for $T_P > 0.017029$, a different coexistence equilibrium is stable

is very briefly stable. Therefore, there is a brief phase of bistability between two coexistence equilibrium. Then, after a Hopf bifurcation, there is a stable limit cycle. Due to the relative values of the two saddle-node bifurcations, there is a phase of bistability between a coexistence equilibrium and a stable limit cycle after the Hopf bifurcation. Note that the value of the Hopf bifurcation point could not be found exactly using MatCont. However, we approximated the Hopf values by finding points on the equilibrium curves where the real part of the complex conjugate pair of eigenvalues was very close to 0 (within 0.011). A sample pair of diagrams is shown in Fig. 4. The values of $\gamma * T_C$ were 0.750 and 0.955 for the first and second combinations respectively. The bifurcations occur at a larger value of T_P for the higher value of $\gamma * T_C$.

As mentioned, the third type of bifurcation diagram pair implies bistability is possible. Indeed, further simulations prove this is true. Consider the parameter regime shown in Fig. 4, i.e., $\gamma = 0.005$, $T_C = 191.0$. The values of the saddle-node bifurcations seem to indicate there should be a region of bistability for $T_P \in [0.02069, 0.02309]$. As shown in Fig. 5, the asymptotic state of the system differs for $T_P = 0.0219$ for different initial conditions. This confirms that bistability does indeed occur in this region, as indicated by Fig. 4.

The fourth type of bifurcation pair occurred for three combinations, with very low γ and between intermediate and high system carbon ($\gamma = 0.005$, $T_C \in \{150, 270, 275\}$). These diagrams are very similar to the third type, with one key difference. The stable limit cycle does not appear to begin until the coexistence equilibrium is unstable, and therefore we do not definitively observe bistability between a coexistence equilibrium and a limit cycle. We see similar bifurcations to type 3: a transcritical bifurcation, a saddle-node bifurcation, a possible Hopf bifurcation, then a saddle-node bifurcation. However, we cannot continue the stable limit cycle with MatCont for a value of T_P less than the later saddle-node bifurcation. Without being able to continue the limit cycle, the only type of bistability we predict is that between the two coexistence

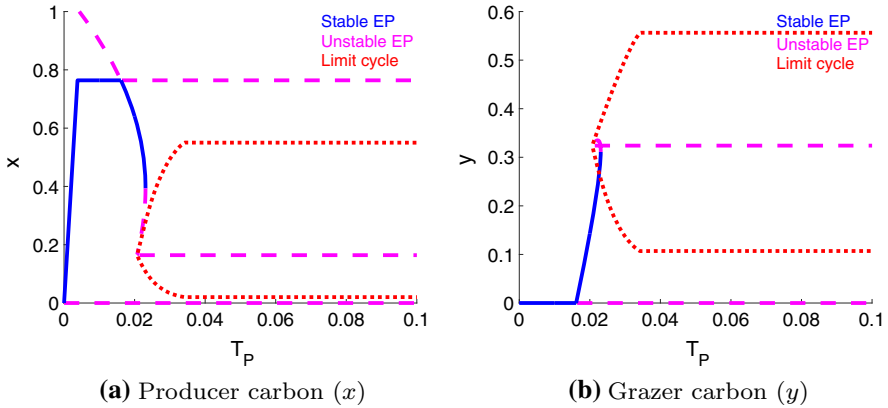


Fig. 4 T_P bifurcation diagrams: $T_C = 191.0$, $\gamma = 0.005$. x is on the left and y is on the right. There is a transcritical bifurcation at $T_P = 0.01612$, a saddle-node bifurcation at $T_P = 0.02069$, and another saddle-node bifurcation at $T_P = 0.02309$. There is also likely a Hopf bifurcation very close to $T_P = 0.02070$ ($Re(\lambda) = 0.006163$). For $T_P < 0.01612$, a grazer extinction equilibrium is stable; for $0.01612 < T_P < 0.02309$, a coexistence equilibrium is feasible and stable; for $0.02069 < T_P < 0.02070$, an additional coexistence equilibrium is stable; and for $T_P > 0.02070$, there is a stable limit cycle. There is bistability between equilibria for $T_P \in (0.02069, 0.02070)$ and between an equilibrium and a limit cycle for $T_P \in (0.02070, 0.2309)$

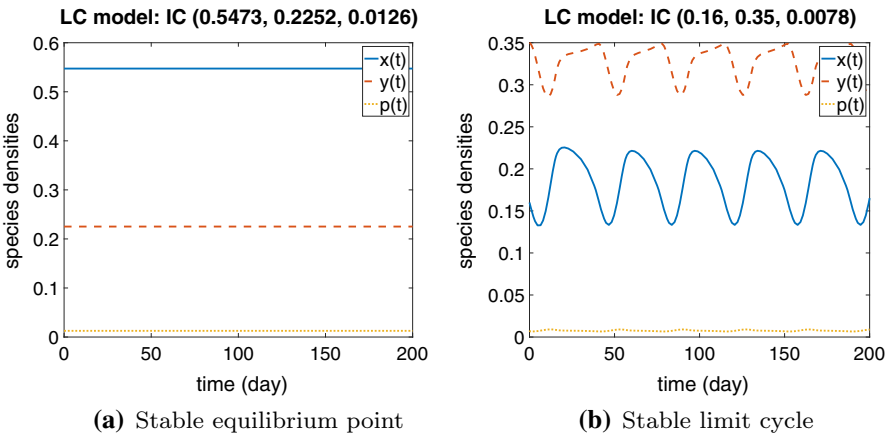


Fig. 5 Bistable states for the limiting case of the model, with $T_C = 191.0$, $T_P = 0.0219$, $\gamma = 0.005$, and two distinct initial conditions. For $(x(0), y(0), p(0)) = (0.5473, 0.2252, 0.0126)$, the coexistence equilibrium point is stable; for $(x(0), y(0), p(0)) = (0.16, 0.35, 0.0078)$, coexistence oscillations are stable

equilibria between the first saddle-node bifurcation and the approximate Hopf bifurcation point. Example diagrams of this type are shown in Fig. 6. Here, $\gamma * T_C$ was in $\{0.75, 1.35, 1.375\}$. For higher values of T_C (and thus $\gamma * T_C$), the bifurcations occurred at a higher value of T_P .

The fifth type of diagram pair occurred for the 13 remaining combinations of γ and T_C examined, with $\gamma * T_C$ ranging from 1.45924 to 172.02988. Again, we could not extend the limit cycle beyond the second saddle-node bifurcation. Note that for all of

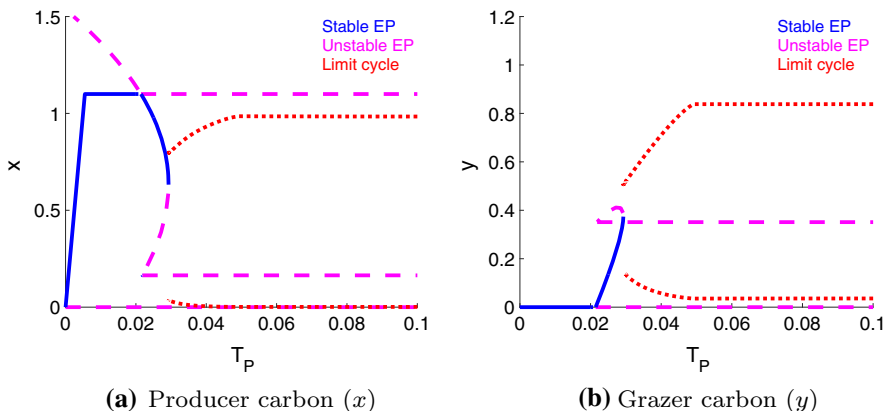


Fig. 6 T_P bifurcation diagrams: $T_C = 275.0$, $\gamma = 0.005$. x is on the left and y is on the right. There is a transcritical bifurcation at $T_P = 0.02144$, a saddle-node bifurcation at $T_P = 0.02188$, and another saddle-node bifurcation at $T_P = 0.02928$. There is also likely a Hopf bifurcation very close to $T_P = 0.02189$ ($Re(\lambda) = -0.000996$). For $T_P < 0.02144$, a grazer extinction equilibrium is stable; for $0.02144 < T_P < 0.02928$, a coexistence equilibrium is feasible and stable; for $0.02188 < T_P < 0.02189$, an additional coexistence equilibrium may be stable; and for $T_P > 0.02928$, there is a stable limit cycle. There may be bistability, first between two coexistence equilibria and then between a coexistence equilibrium and a limit cycle

these combinations, the order of the bifurcation values is saddle-node, transcritical, saddle-node, whereas in the fourth type, the transcritical bifurcation occurs at a lower value of T_P than both saddle-node bifurcations. Hence, the bistability observed is between a grazer extinction equilibrium and a coexistence equilibrium, and then there may be bistability between a grazer extinction equilibrium and a limit cycle, and then between a coexistence equilibrium and a limit cycle. Using the bifurcation values observed, we realize the transcritical bifurcation value fits a linear regression, with the value approximately equal to $0.0094 * \gamma * T_C + 0.0259$, with $R^2 = 0.9976$; the larger saddle-node bifurcation value also fits a linear regression, with the value approximately equal to $0.0119 * \gamma * T_C + 0.0321$, with $R^2 = 0.9981$. Comparatively, with the exception of the combination shown in Fig. 7, the other saddle-node bifurcations occur at $T_P = 0.022325272 \pm 0.00000028$; the Hopf points with a $|Re(\lambda)| < 0.011$ occur at $T_P = 0.02232551 \pm 0.00000039$.

The value that determines which diagram pair a parameter combination corresponds to may be $\gamma * T_C$. For the five different types, the values of $\gamma * T_C$ are: (1) $\{0.25, 0.375\}$; (2) $\{0.45, 0.491\}$; (3) $\{0.750248, 0.955\}$; (4) $\{0.75, 1.35, 1.375\}$; and (5) $[1.45924, 172.02988]$. There may be threshold values of $\gamma * T_C$ that determine the bifurcations observed.

4.2.2 Total system carbon

For total system carbon, T_C , we observed four different types of diagram pairs.

The first type of bifurcation diagram pair occurred for low system phosphorus ($T_P = 0.003$). There are no bifurcations. The total system phosphorus is sufficiently

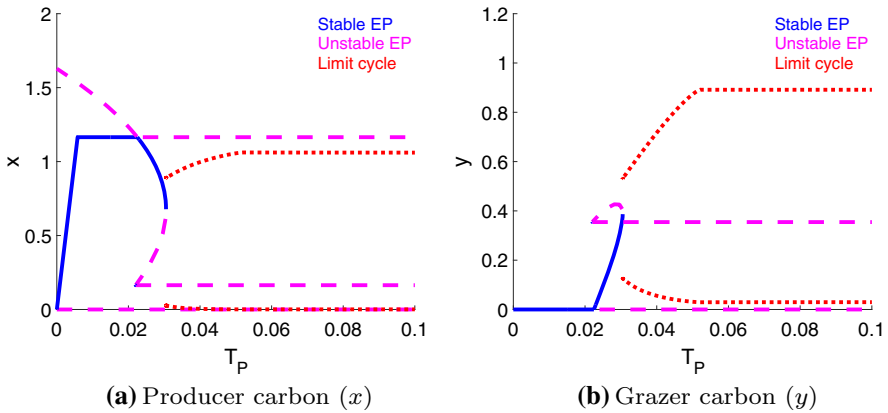


Fig. 7 T_P bifurcation diagrams: $T_C = 191.0$, $\gamma = 0.00764$. x is on the left and y is on the right. There is a transcritical bifurcation at $T_P = 0.02247$, a saddle-node bifurcation at $T_P = 0.022036$, and another saddle-node bifurcation at $T_P = 0.03051$. There also may be a Hopf bifurcation very close to $T_P = 0.022038$ ($Re(\lambda) = -0.00930$). For $T_P < 0.02247$, a grazer extinction equilibrium is stable; for $0.022036 < T_P < 0.022038$, there is a stable coexistence equilibrium; for $0.02247 < T_P < 0.03051$, another coexistence equilibrium is feasible and stable; and for $T_P > 0.03051$, there is a stable limit cycle. There is bistability between a grazer extinction equilibrium and a coexistence equilibrium for $0.022036 < T_P < 0.022038$, and there may be bistability between a limit cycle and a grazer extinction equilibrium and then a coexistence equilibrium

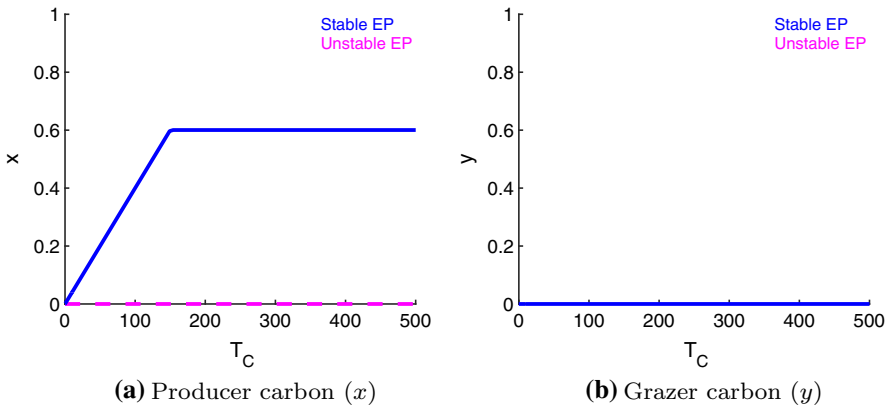


Fig. 8 T_C bifurcation diagrams: $T_P = 0.003$, $\gamma = 0.005$. x is on the left and y is on the right. There are no bifurcations. A grazer extinction equilibrium is stable throughout

low that the grazer extinction equilibrium is stable throughout, as shown in Fig. 8. The producer carbon (x) equilibrium value plateaus as total carbon increases when the producer’s growth switches from being carbon limited to being phosphorus limited.

The second type of bifurcation diagram pair occurred for very low γ and several levels between low and intermediate system phosphorus ($\gamma = 0.005$, $T_P \in \{0.007, 0.010, 0.018\}$). For the lowest values of T_C , a grazer extinction equilibrium is stable. Then, after a transcritical bifurcation, a coexistence equilibrium becomes stable and the grazer extinction equilibrium becomes unstable. This behaviour con-

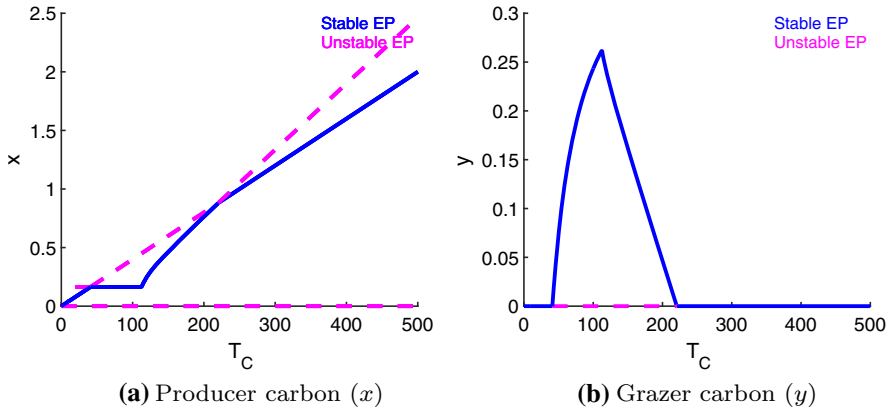


Fig. 9 T_C bifurcation diagrams: $T_P = 0.018$, $\gamma = 0.005$. x is on the left and y is on the right. There are two transcritical bifurcations at $T_C = 41.04412$ and 220.65837

tinues until another transcritical bifurcation occurs, after which the grazer extinction equilibrium is stable once more and the coexistence equilibrium unstable. A sample pair of diagrams is shown in Fig. 9.

The third type of bifurcation diagram pair for total carbon was observed only for one specific combination of parameters, selected using the total phosphorus diagrams. The pair, shown in Fig. 10, corresponds to $\gamma = 0.005$ and $T_P = 0.022325$. For very low T_C , a grazer extinction equilibrium is stable. Then, after a transcritical bifurcation, a coexistence equilibrium becomes stable. This equilibrium point remains stable until a Hopf bifurcation point, at which a limit cycle becomes stable. There is a saddle-node bifurcation, after which another coexistence equilibrium becomes stable. After a transcritical bifurcation, the second coexistence equilibrium becomes unstable and the grazer extinction equilibrium becomes stable once more. Then, after another Hopf bifurcation, the first coexistence equilibrium becomes stable once more. The limit cycle could not be continued for larger values of T_C , despite the second Hopf bifurcation seeming to imply it should be stable until the second Hopf bifurcation. Around $T_C = 198$, there is a limit point cycle, as well as a neutral saddle cycle, and the period becomes incredibly large. However, we still clearly observe bistability. There is bistability between a limit cycle and a coexistence equilibrium between the saddle-node bifurcation and the value of T_C at which the limit cycle could not be continued. There is also bistability between a coexistence equilibrium and a grazer extinction equilibrium after the second Hopf point.

The fourth type of bifurcation diagram pair occurred for intermediate to high system phosphorus ($T_P \in \{0.025, 0.030, 0.300\}$). For the lowest values of T_C , a grazer extinction equilibrium is stable. Then, after a transcritical bifurcation, the grazer extinction equilibrium becomes unstable and a coexistence equilibrium becomes feasible and stable. This coexistence equilibrium becomes unstable at a Hopf bifurcation, at which point a stable limit cycle appears. The amplitude of this limit cycle increases and it remains stable until a saddle-node bifurcation. At the saddle-node bifurcation, the limit cycle becomes unstable or disappears and we see different stable and unstable

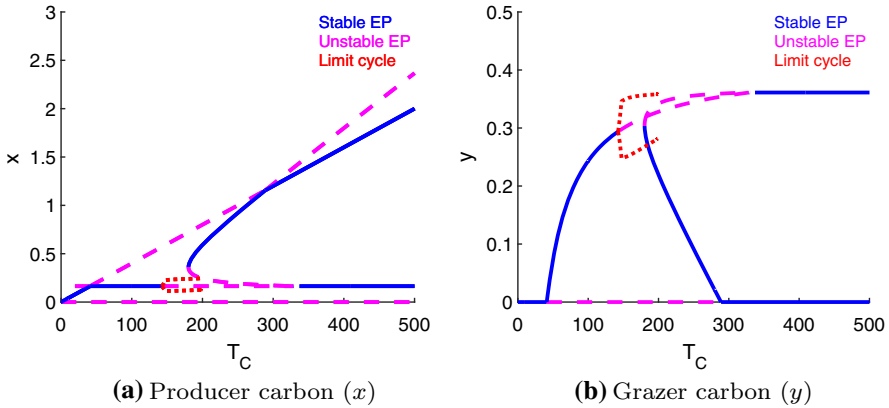


Fig. 10 T_C bifurcation diagrams: $T_P = 0.022325$, $\gamma = 0.005$. x is on the left and y is on the right. There is a transcritical bifurcation at $T_C = 41.04412$, a Hopf bifurcation at $T_C = 144.58605$, a saddle-node bifurcation at $T_C = 180.21078$, a second transcritical bifurcation at $T_C = 288.88353$, and a second Hopf bifurcation at $T_C = 328.49123$. The grazer extinction equilibrium is stable for $T_C < 41.04412$ and $T_C > 288.88353$. The first coexistence equilibrium is stable for $41.04412 < T_C < 144.58605$ and for $T_C > 328.49123$. The second coexistence equilibrium is stable for $180.21078 < T_C < 288.88353$. The limit cycle is stable for at least $144.58605 < T_C < 198$

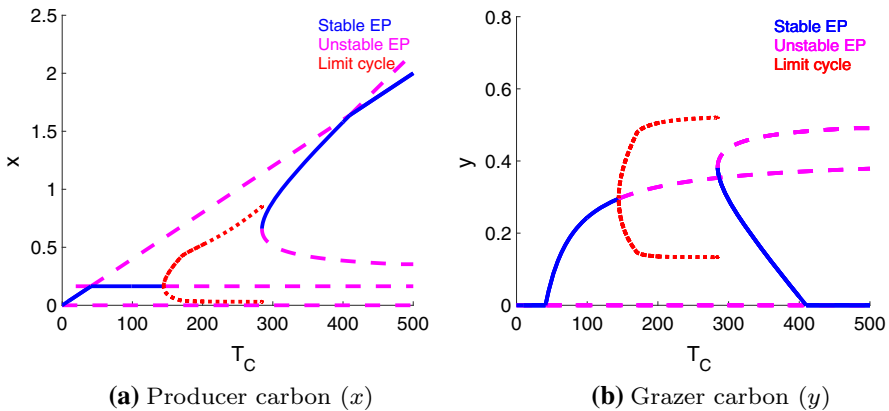
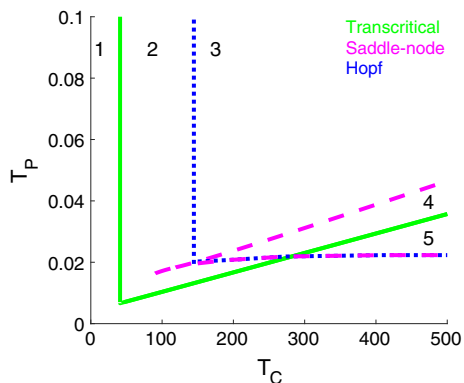


Fig. 11 T_C bifurcation diagrams: $T_P = 0.030$, $\gamma = 0.005$. x is on the left and y is on the right. There is a transcritical bifurcation at $T_C = 41.04412$, a Hopf bifurcation at $T_C = 144.58604$, a saddle-node bifurcation at $T_C = 284.55386$, and another transcritical bifurcation at $T_C = 409.92590$. For $T_C < 41.04412$, a grazer extinction equilibrium is stable; for $41.04412 < T_C < 144.58604$, a coexistence equilibrium is feasible and stable; for $144.58604 < T_C < 284.55386$, there is a stable limit cycle; for $284.55386 < T_C < 409.92590$, a different coexistence equilibrium is stable; and for $T_C > 409.92590$, the grazer extinction equilibrium is stable again

coexistence equilibrium branches appear. The stable second coexistence equilibrium remains stable until a second transcritical bifurcation point, at which the coexistence equilibrium becomes unstable and the grazer extinction equilibrium becomes stable once more. A sample diagram is shown in Fig. 11.

Fig. 12 Two parameter bifurcation diagram for $\gamma = 0.005$ (very low γ). The stable behaviours in the regions are: (1) grazer extinction equilibrium; (2) coexistence equilibrium; (3) coexistence oscillations; (4) coexistence equilibrium or bistability between a coexistence equilibrium and a limit cycle; (5) grazer extinction equilibrium or bistability between a coexistence equilibrium and a grazer extinction equilibrium



While the first transcritical bifurcation point and the Hopf bifurcation point occur at fairly consistent values for the various T_P values for a given γ , the saddle-node bifurcation and the second transcritical bifurcation point occur at different values for different T_P . For the saddle-node bifurcation point, the bifurcation value for each γ for high phosphorus is between 13.1928843 and 13.2105029 times the value for intermediate phosphorus (average 13.2058894). For the second transcritical bifurcation point, the bifurcation value for each γ for high phosphorus is between 11.3850574 and 11.3855909 times the value for intermediate phosphorus (roughly 11.3850574 for all γ except the highest). For all bifurcation points for T_C , the values decrease as γ increases.

4.3 Two parameter bifurcation analysis

Two parameter bifurcation diagrams were also generated using MatCont (Dhooge et al. 2008) for the limiting closed case of the model ($\alpha = 0$, $\rho(C) = 1$). A diagram was produced for each value of γ explored in the previous section.

In general, the two parameter bifurcation diagrams look very similar to each other. The primary difference beyond the scale of T_C lies in the codimension 2 bifurcations MatCont found. For very low γ ($\gamma = 0.005$), there is a cusp point along the saddle-node branch, at $T_C = 97.09174$ and $T_P = 0.016942$. For low γ ($\gamma = 0.00764$), there is a Generalized Hopf point at $T_C = 94.82381$ and $T_P = 0.019545$. A sample two parameter bifurcation diagram is shown in Fig. 12.

Several of the curves in this diagram were added manually using the bifurcation values found in the one parameter analysis, since several of the curves could not be continued in MatCont. The values for the more horizontal Hopf curve were all approximate, and there may be an unlabelled region between the horizontal Hopf and saddle-node curves, which seemingly intersect several times.

We observe that for very low values of T_P and T_C , we consistently see extinction of the grazer, labelled with 1 in Fig. 12. After the transcritical bifurcation, we primarily observe a stable coexistence equilibrium (region 2), until the Hopf bifurcation, after which we observe a stable limit cycle (region 3). There are two regions with more complicated dynamics. Region 4 is bounded by a saddle-node, a Hopf, and transcritical

bifurcation curve. The total phosphorus one parameter diagrams seem to indicate that for this region, there should be bistability between a coexistence equilibrium and a stable limit cycle. Comparatively, the total carbon diagrams primarily demonstrated only a stable coexistence equilibrium, with the exception of $T_P = 0.0022325$ (see Fig. 10). Region 5 is bounded by a Hopf and a transcritical bifurcation curve. Here the phosphorus diagrams demonstrated bistability between a coexistence and a grazer extinction equilibrium, while all of the carbon diagrams exhibited grazer extinction, except $T_P = 0.0022325$. Given the contradictory results, there may be subcases that are not shown due to extremely high sensitivity of the model simulations.

There is an interesting transition across the saddle-node bifurcation curve. For T_C larger than the Hopf bifurcation value, the saddle-node bifurcation curves approximate where one coexistence equilibrium becomes stable immediately before a Hopf bifurcation (lower saddle-node curve), and where the other coexistence equilibrium becomes unstable (higher saddle-node curve). However, for the brief portion of the saddle-node bifurcation curve occurring at T_C less than the Hopf bifurcation value, a coexistence equilibrium is stable both before and after this bifurcation. Consider, for example, $T_C = 98.2$. The bifurcation is now a change in which coexistence equilibrium is stable. There should be an additional saddle-node curve very close to the one shown, where the saddle produced after the first saddle-node bifurcation collides with the new stable coexistence equilibrium. The difference in coexistence equilibria is likely due to a change in which factor is limiting for the producer and/or grazer, since the equilibria are different for different limiting factors.

5 Discussion

There are many ecological stoichiometry models which have been developed to explicitly track the impacts of multiple elements on ecological interactions. However, these models usually assume that the system is completely open to carbon. This limits their usefulness in studying the potential impacts of increased atmospheric carbon dioxide concentration on food webs, since the availability of carbon for photosynthesis is not modelled. It has been proven that an increase in atmospheric carbon dioxide can cause an increase in the rate of photosynthesis, and a corresponding increase in growth and production of autotrophs (Ainsworth and Rogers 2007). When producer-grazer systems are closed to nutrients such as phosphorus or nitrogen, the resulting decrease in nutrient levels in the producer can impact the growth of the grazers, which tend to have higher, more rigid nutrient requirements (Sterner and Elser 2002; Urabe et al. 2003).

In order to study the potential impacts of the current global increase in atmospheric carbon dioxide on producer-grazer systems, a model was developed to allow for explicit consideration of carbon availability. The model was based on the WKL model (Wang et al. 2008), which was itself based on the LKE model (Loladze et al. 2000). Light was removed as a limiting factor for producer growth, and replaced with a carbon-dependent carrying capacity ($h(C)$) for producer growth in the minimum term. In addition, the model incorporates explicit consideration of producer respira-

tion, including the reduction in photorespiration rate observed due to elevated CO_2 , and allowance for some degree of openness in the system for carbon.

A limiting case of the model, in which the reduction in photorespiration rate and allowance for openness were not incorporated ($\rho(C) = 1$, $\alpha = 0$), was analyzed. For this case, there is a biologically meaningful region which is forward invariant. There is also a sufficient condition for global asymptotic stability of the total extinction equilibrium, which depends on several parameters, including the total phosphorus in the system. If we assume Holling type I functional responses for f and g , there are between 1 and 3 boundary equilibria, and there may also be coexistence equilibria. When f and g take the form of Holling type II functional responses, there are between 1 and 4 boundary equilibria, and potentially coexistence equilibria. There are many complicated conditions for stability of these equilibria, which depend on which factors are limiting for producer and grazer growth at the equilibria.

The two parameters examined in the bifurcation analysis of the limiting case were the total nutrients in the closed system, T_C and T_P . These parameters contribute to determining the limiting factors for growth of the producer and grazer. Bifurcation analysis generally demonstrated sequential limitation by the different growth factors for the producer, with the general pattern being stability of a grazer extinction equilibrium, then a coexistence equilibrium, and then a limit cycle. Occasionally the system also transitions to a second stable coexistence equilibrium via a saddle-node bifurcation, and then returns to the grazer extinction equilibrium. In particular, these additional bifurcations occurred for intermediate to high phosphorus and using T_C as the bifurcation parameter.

Similar to the bifurcation diagrams for K in Wang et al. (2008), the grazers go extinct at low T_C due to insufficient quantity of food, and they go extinct at high T_C due to insufficient quality of food. Therefore, increased levels of atmospheric carbon dioxide are expected to cause grazer extinction due to insufficient quality of food when soil nutrients are limiting. Additionally, given the plateaus in x as T_C increases in the total carbon bifurcation diagrams, this model suggests that there is a limit to carbon sequestration determined by availability of soil nutrients, as expected given the application of Liebig's Law of the Minimum.

Simulations were used to examine the impacts on the system of a non-constant producer respiration rate ($\rho(C) \neq 1$) or transfer of carbon with the environment ($\alpha > 0$), as well as those of the potentially limiting parameters. In general, the combinations examined either produced a grazer extinction equilibrium, a coexistence equilibrium, or coexistence oscillations. In certain cases, bistability between a coexistence equilibrium and a limit cycle was observed. Overall, the dynamics seemed to be very similar regardless of the $\rho(C)$ or α used. Even though the differences were minimal, the most distinct model at high carbon was observed with non-constant $\rho(C)$.

There are limitations for both this model and its analysis. This model relies on an assumption of independent colimitation of producer growth by carbon and phosphorus. There is evidence for independent colimitation by carbon and phosphorus (Spijkerman et al. 2011). However, no conclusive evidence was found for colimitation of producer growth by light and carbon, and thus we assumed here that light was sufficient. This simplifying assumption limits applicability of the results. There is certainly empirical evidence for increased growth due to elevated carbon dioxide of plants growing in

shade (Körner 2009; Lovelock et al. 1996; Würth et al. 1998). This is likely because elevated carbon dioxide increases light use efficiency, partially because the increase in carbon fixation due to reduction of photorespiration requires no additional light (Drake et al. 1997), as well as because elevated CO₂ can decrease the light compensation point of a leaf (Long and Drake 1991). This evidence supports the theory that colimitation of light and carbon may not be independent, and thus, there may be more complicated dynamics observed naturally that cannot be covered by this model.

Additional impacts of increased carbon dioxide on producers that were not incorporated into this model include changes in carbon allocation, changes in light or nutrient efficiencies, changes in dark respiration (mitochondrial/cellular respiration), and changes in decomposition rates. There is contradictory evidence for changes in carbon allocation. Some evidence seems to support an increase in plant root:shoot ratio and leaf area (Elser et al. 2010); some supports no stimulation in foliage (Drake et al. 1997); and some suggests an increase in fine root allocation at the expense of wood and leaves, or increase in wood allocation at the expense of leaves (De Kauwe et al. 2013; Pugh et al. 2016). Similarly, the evidence for changes in respiration is inconsistent, with plants grown in elevated carbon dioxide exhibiting an increase, decrease, or no significant change in dark respiration rates (Leakey et al. 2009). Lastly, incorporation of changes in the rates of decomposition in this model, such as those discussed in de Graaff et al. (2006), would require relaxation of the assumption that carbon and phosphorus released by the producer and grazer is immediately available for use.

There are many opportunities for future work for both this specific research question and this model. The vast majority of analysis completed is for the limiting closed case ($\alpha = 0$, $\rho(C) = 1$), and thus the more complicated cases remain to be analyzed. In particular, it would be interesting to consider the impact of the “openness” parameter (α). Additionally, a more evidence-based method of selecting $\rho(C)$, as well as modification to see at what point dynamics shift, may allow us to better understand the impacts of increased global atmospheric carbon dioxide concentration on producer-grazer systems. Also, the bifurcation analysis completed is local. Even with the variety of parameter regimes considered, there are likely other behaviours that would be observed in natural systems that are not explored here. Further investigation of the regions that demonstrated bistability in the two parameter diagrams may also be beneficial.

Modelling wise, incorporation of more factors such as those described above may be interesting. In addition, a model considering nitrogen instead of phosphorus as a limiting nutrient could be illuminating. Nitrogen is a commonly limiting nutrient in terrestrial systems (Sternner and Elser 2002), and it may be more closely related to photosynthesis since up to 25% of leaf nitrogen is used in Rubisco, the carbon fixation enzyme, and increased efficiency of Rubisco due to increased atmospheric carbon dioxide concentration causes a reduction in allocation of nitrogen to Rubisco (Drake et al. 1997).

An additional research question that could be addressed using this model is investigation of dynamic shifts due to elevated carbon dioxide specifically for terrestrial versus aquatic systems, similar to Davies and Wang (2020). Another question would involve investigation of the impact of elevated atmospheric carbon dioxide concentration on competition between grazers with different nutrient requirements.

Lastly, this model would likely benefit from data fitting and validation. As it stands, many of the parameter regions examined are primarily theoretical. It would be valuable to apply data from free-air carbon enrichment experiments, as well as experiments such as those conducted by Urabe et al. (2003) to understand which parameter regions require further study.

Acknowledgements This research is partially supported by an NSERC Discovery Grant RGPIN-2020-03911 and an NSERC Accelerator Grant RGPAS-2020-00090.

Appendix A

This appendix contains the proof of Theorem 1.

Proof Let $X(t) \equiv (x(t), y(t), p(t))$ be a solution of Eqs. (6)–(8) with initial conditions in Ω . Then, $0 < x(0) < \min\{T_P/q, h(T_C)\}$, $0 < y(0)$, $0 < p(0)$, $p(0) + \theta y(0) < T_P$, and $x(0) + y(0) < T_C$. Assume for the sake of contradiction that there is time $t_1 > 0$ such that $X(t)$ touches or crosses the boundary of $\bar{\Omega}$ (closure of Ω) for the first time. Therefore, $(x(t), y(t), p(t)) \in \Omega$ for $0 \leq t < t_1$. We now consider cases for which part of the boundary of $\bar{\Omega}$ $X(t_1)$ lies on.

Case 1 $x(t_1) = 0$ but $p(t_1) \neq 0$. Since $(x(t), y(t), p(t)) \in \Omega$ for $0 \leq t < t_1$, then $0 < p(t)$ and $p(t) + \theta y(t) \leq T_P$ for $0 \leq t \leq t_1$. Also, all parameters are assumed to be positive. Therefore, $y(t) \leq T_P/\theta - p(t)/\theta < T_P/\theta$ for $0 \leq t \leq t_1$. Let $p_1 = \min\{p(t) : t \in [0, t_1]\} > 0$, $x_1 = \max\{x(t) : t \in [0, t_1]\} > 0$, and $y_1 = \max\{y(t) : t \in [0, t_1]\} > 0$. Both x_1 and y_1 are guaranteed to exist since the initial conditions are in Ω and thus are positive. Then for $0 \leq t \leq t_1$, we have (using Eq. 6)

$$\begin{aligned} \frac{dx}{dt} &= rx \left(1 - \frac{x}{\min\{p/q, h(T_C - x - y)\}} \right) - f(x)y - l_x x \\ &\geq rx \left(1 - \frac{\min\{T_P/q, h(T_C)\}}{\min\{p_1/q, h(T_C - x_1 - y_1)\}} \right) - f'(0)(T/\theta)x - l_x x \\ &= \left[r \left(1 - \frac{\min\{T_P/q, h(T_C)\}}{\min\{p_1/q, h(T_C - x_1 - y_1)\}} \right) - f'(0)(T/\theta) - l_x \right] x \equiv \mu x, \end{aligned}$$

where μ is a constant. Then, $x(t) \geq x(0)e^{\mu t}$ for $0 \leq t \leq t_1$, which implies $x(t_1) \geq x(0)e^{\mu t_1} > 0$, which is a contradiction.

Case 2 $x(t_1) = \min\{T_P/q, h(T_C)\}$. Since $(x(t), y(t), p(t)) \in \Omega$ for $0 \leq t < t_1$, we know $0 \leq y(t)$ and $p(t) + \theta y(t) \leq T_P$ for $0 \leq t \leq t_1$. Therefore, $p(t) \leq T_P - \theta y(t) \leq T_P$ for $0 \leq t \leq t_1$. Clearly $T_C - x(t) - y(t) \leq T_C$ for $x(t), y(t) \geq 0$. Since $h(C)$ is non-decreasing, then $h(T_C - x(t) - y(t)) \leq h(T_C)$ for $x(t), y(t) \geq 0$. Hence, for $0 \leq t \leq t_1$, we have

$$\frac{dx}{dt} = rx \left(1 - \frac{x}{\min\{p/q, h(T_C - x - y)\}} \right) - f(x)y - l_x x$$

$$\leq rx \left(1 - \frac{x}{\min\{T_P/q, h(T_C)\}} \right).$$

Note that the right hand side is logistic growth in x with the carrying capacity given by $\min\{T_P/q, h(T_C)\}$. The standard comparison argument yields that $x(t) < \min\{T_P/q, h(T_C)\}$ for all $0 \leq t \leq t_1$, a contradiction.

Case 3 $y(t_1) = 0$. For $0 \leq t \leq t_1$, we have from Eq. (7)

$$\begin{aligned} \frac{dy}{dt} &= \hat{e} \min \left\{ 1, \frac{p/x}{\theta} \right\} f(x)y - \hat{d}y - l_y y \\ &= \left(\hat{e} \min \left\{ 1, \frac{p/x}{\theta} \right\} f(x) - \hat{d} - l_y \right) y \geq -(\hat{d} + l_y)y \end{aligned}$$

since all parameters are assumed to be positive; $f(0) = 0, f'(x) > 0, f''(x) \leq 0$ for $x \geq 0$; and $(x(t), y(t), p(t)) \in \Omega$ for $0 \leq t < t_1$. Hence, $y(t) \geq y(0)e^{-(\hat{d}+l_y)t} > 0$ for $0 \leq t \leq t_1$, a contradiction.

Case 4 $p(t_1) = 0$. Since $(x(t), y(t), p(t)) \in \Omega$ for $0 \leq t < t_1$, we know $p(t) + \theta y(t) \leq T_P$ for $0 \leq t \leq t_1$. Therefore, $T_P - p(t) - \theta y(t) \geq 0$ for $0 \leq t \leq t_1$, and since we assume that in general $g(0) = 0$ and $g'(P) > 0$ for $P \geq 0$, then $g(T_P - p(t) - \theta y(t)) \geq 0$ for $0 \leq t \leq t_1$.

Also, since $0 \leq p(t)$ and $p(t) + \theta y(t) \leq T_P$ for $0 \leq t \leq t_1$, then $y(t) \leq T_P/\theta - p(t)/\theta \leq T_P/\theta$ for $0 \leq t \leq t_1$, and therefore $-T_P/\theta \leq -y(t)$.

Thus, for $0 \leq t \leq t_1$, we have from Eq. (8)

$$\begin{aligned} \frac{dp}{dt} &= g(T_P - p - \theta y)x - \frac{P}{x} f(x)y - dp \geq -\frac{P}{x} f(x)y - dp \\ &\geq [-f'(0)(T_P/\theta) - d]p \equiv \nu p, \end{aligned}$$

where ν is a constant. Thus, $p(t) \geq p(0)e^{\nu t} > 0$ for $0 \leq t \leq t_1$, a contradiction.

Case 5 $p(t_1) + \theta y(t_1) = T_P$. Let $z(t) = T_P - p(t) - \theta y(t)$. Since $p(t_1) + \theta y(t_1) = T_P$, then $z(t_1) = 0$. Also, since t_1 is assumed to be the first time that $X(t)$ touches or crosses the boundary of $\bar{\Omega}$, then $p(t) + \theta y(t) < T_P$ for $0 \leq t < t_1$ and thus $z(t) > 0$ for $0 \leq t < t_1$. Then for $0 \leq t \leq t_1$, we have

$$\begin{aligned} \frac{dz}{dt} &= \frac{d}{dt}(T_P - p - \theta y) = \frac{d}{dt}T_P - \frac{dp}{dt} - \theta \frac{dy}{dt} = -\frac{dp}{dt} - \theta \frac{dy}{dt} \\ &= -\left(g(T_P - p - \theta y)x - \frac{P}{x} f(x)y - dp \right) - \theta \left(\hat{e} \min \left\{ 1, \frac{p/x}{\theta} \right\} f(x)y - \hat{d}y - l_y y \right) \\ &= -g(T_P - p - \theta y)x + \frac{P}{x} f(x)y + dp - \theta \hat{e} \min \left\{ 1, \frac{p/x}{\theta} \right\} f(x)y + \theta \hat{d}y + \theta l_y y \\ &\geq -g(T_P - p - \theta y)x + dp + \theta \hat{d}y + \theta l_y y \geq -g(z)x + dp + (\hat{d} + l_y)\theta y \\ &\geq -g'(0)z \min\{T_P/q, h(T_C)\} + \min\{d, \hat{d} + l_y\}(T_P - z) \\ &= \min\{d, \hat{d} + l_y\}T_P - [g'(0)\min\{T_P/q, h(T_C)\} + \min\{d, \hat{d} + l_y\}]z \equiv \tilde{\mu} - \tilde{\nu}z, \end{aligned}$$

where $\tilde{u} > 0$ and $\tilde{v} > 0$ are constant. Thus $z(t) \geq e^{-\tilde{v}t}z(0) > 0$ for $0 \leq t \leq t_1$, a contradiction.

Case 6 $x(t_1) + y(t_1) = T_C$. Consider the limit of dx/dt as $t \rightarrow t_1$:

$$\begin{aligned} \lim_{t \rightarrow t_1} \frac{dx}{dt} &= \lim_{t \rightarrow t_1} \left[rx \left(1 - \frac{x}{\min\{p/q, h(T_C - x - y)\}} \right) - f(x)y - l_x x \right] \\ &= \lim_{t \rightarrow t_1} rx \left(1 - \frac{x}{\min\{p/q, h(T_C - x - y)\}} \right) - \lim_{t \rightarrow t_1} f(x)y - \lim_{t \rightarrow t_1} l_x x \\ &= rx(t_1) - \lim_{t \rightarrow t_1} \frac{rx^2}{\min\{p/q, h(T_C - x - y)\}} - f(x(t_1))y(t_1) - l_x x(t_1). \end{aligned}$$

Since $h(0) = 0$, then the limit as $t \rightarrow t_1$ of $\min\{p/q, h(T_C - x - y)\}$ is 0. However, $x(t_1) > 0$. Therefore, as $t \rightarrow t_1$, the limit of dx/dt is $-\infty$. Clearly this implies that $dy/dt \rightarrow -\infty$ as $t \rightarrow t_1$. But then as $t \rightarrow t_1$, $x(t) + y(t) \rightarrow -\infty$, a contradiction. \square

Appendix B

This appendix contains all the necessary information to find the equilibria assuming Holling type I functional responses for f and g . In addition, we assume $\alpha = 0$ and $\rho(C) = 1$.

Substituting $f(x) = cx$, $g(P) = \hat{c}P$ and $h(C) = \gamma C$ into Eqs. (6)–(8), we get the following system:

$$\begin{aligned} \frac{dx}{dt} &= rx \left(1 - \frac{x}{\min\{p/q, \gamma(T_C - x - y)\}} \right) - cxy - l_x x, \\ \frac{dy}{dt} &= \hat{e} \min \left\{ 1, \frac{p/x}{\theta} \right\} cxy - \hat{d}y - l_y y, \\ \frac{dp}{dt} &= \hat{c}(T_P - p - \theta y)x - \frac{p}{x}cxy - dp. \end{aligned}$$

Equilibria satisfy

$$\begin{aligned} 0 &= \bar{x} \left(r \left(1 - \frac{\bar{x}}{\min\{\bar{p}/q, \gamma(T_C - \bar{x} - \bar{y})\}} \right) - c\bar{y} - l_x \right) \equiv \bar{x}F(\bar{x}, \bar{y}, \bar{p}), \\ 0 &= \bar{y} \left(\hat{e} \min \left\{ 1, \frac{\bar{p}/\bar{x}}{\theta} \right\} c\bar{x} - \hat{d} - l_y \right) \equiv \bar{y}G(\bar{x}, \bar{y}, \bar{p}), \\ 0 &= \hat{c}(T_P - \bar{p} - \theta\bar{y})\bar{x} - c\bar{p}\bar{y} - d\bar{p} \equiv H(\bar{x}, \bar{y}, \bar{p}). \end{aligned}$$

Clearly the trivial extinction equilibrium $E_0 = (0, 0, 0)$ is a possible solution of the above. We can also explicitly find the forms of the grazer extinction equilibria. The grazer extinction equilibria always take the form $(\bar{x}, 0, \bar{p})$, where \bar{x} and \bar{p} are decided by what is limiting the producer and other parameter-based conditions.

When the producer is phosphorus limited at equilibrium ($\bar{p}/q \leq \gamma(T_C - \bar{x})$), a grazer extinction equilibrium is given by $(\bar{x}, 0, \bar{p})$ where

$$\bar{x} = \frac{\hat{c}T_P(r - l_x) - dq r}{\hat{c}q r},$$

$$\bar{p} = \frac{\hat{c}T_P(r - l_x) - dq r}{\hat{c}(r - l_x)}.$$

We assume all parameters are positive. For $\bar{x} \geq 0$, we need $\hat{c}T_P(r - l_x) - dq r \geq 0$. Then, for $\bar{p} \geq 0$, we need $r - l_x > 0$.

When the producer is carbon limited at equilibrium ($\gamma(T_C - \bar{x}) \leq \bar{p}/q$), we have $(\bar{x}, 0, \bar{p})$ where

$$\bar{x} = \frac{\gamma T_C(r - l_x)}{r + \gamma r - \gamma l_x},$$

$$\bar{p} = \frac{\hat{c}\gamma T_C T_P(r - l_x)}{\hat{c}\gamma T_C(r - l_x) + d(r + \gamma r - \gamma l_x)}.$$

For this equilibrium to be biologically feasible and not equal to E_0 , we require either $r - l_x > 0$ and $r + \gamma r - \gamma l_x > 0$, or $r - l_x < 0$ and $r + \gamma r - \gamma l_x < 0$.

To determine parameter-based conditions for which grazer extinction equilibria are present, we substitute the equilibria into $\bar{p}/q = \gamma(T_C - \bar{x})$. With some rearrangement, we find that for both the phosphorus and carbon limited equilibria, $\bar{p}/q = \gamma(T_C - \bar{x})$ when

$$\hat{c}\gamma T_P(r - l_x)^2 + (\hat{c}T_P - \hat{c}q\gamma T_C - dq\gamma)r(r - l_x) - dq r^2 = 0.$$

A grazer extinction equilibrium takes the phosphorus limited form when $\bar{p}/q \leq \gamma(T_C - \bar{x})$, or equivalently,

$$\frac{\hat{c}\gamma T_P(r - l_x)^2 + (\hat{c}T_P - \hat{c}q\gamma T_C - dq\gamma)r(r - l_x) - dq r^2}{\hat{c}q r(r - l_x)} \leq 0.$$

A grazer extinction equilibrium takes the carbon limited form when $\bar{p}/q \geq \gamma(T_C - \bar{x})$, that is,

$$\frac{\hat{c}\gamma T_P(r - l_x)^2 + (\hat{c}T_P - \hat{c}q\gamma T_C - dq\gamma)r(r - l_x) - dq r^2}{(\hat{c}\gamma T_C(r - l_x) + dq(r + \gamma r - \gamma l_x))(r + \gamma r - \gamma l_x)} \geq 0.$$

There may also be coexistence equilibria, which would satisfy

$$0 = r \left(1 - \frac{\bar{x}}{\min\{\bar{p}/q, \gamma(T_C - \bar{x} - \bar{y})\}} \right) - c\bar{y} - l_x = F(\bar{x}, \bar{y}, \bar{p}),$$

$$0 = \hat{e} \min \left\{ 1, \frac{\bar{p}/\bar{x}}{\theta} \right\} c\bar{x} - \hat{d} - l_y = G(\bar{x}, \bar{y}, \bar{p}),$$

$$0 = \hat{c}(T_P - \bar{p} - \theta \bar{y})\bar{x} - c\bar{p}\bar{y} - d\bar{p} = H(\bar{x}, \bar{y}, \bar{p}).$$

Appendix C

This appendix contains all the necessary information to find the equilibria assuming Holling type II functional responses for f and g . In addition, we assume $\alpha = 0$ and $\rho(C) = 1$.

Using $f(x) = cx/(a + x)$, $g(P) = \hat{c}P/(\hat{a} + P)$, and $h(C) = \gamma C$,

$$\begin{aligned} \frac{dx}{dt} &= rx \left(1 - \frac{x}{\min\{p/q, \gamma(T_C - x - y)\}} \right) - \frac{cx}{a + x}y - l_x x, \\ \frac{dy}{dt} &= \hat{e} \min \left\{ 1, \frac{p/x}{\theta} \right\} \frac{cx}{a + x}y - \hat{d}y - l_y y, \\ \frac{dp}{dt} &= \frac{\hat{c}(T_P - p - \theta y)}{\hat{a} + T_P - p - \theta y}x - \frac{p}{x} \frac{cx}{a + x}y - dp. \end{aligned}$$

Equilibria satisfy

$$\begin{aligned} 0 &= \bar{x} \left(r \left(1 - \frac{\bar{x}}{\min\{\bar{p}/q, \gamma(T_C - \bar{x} - \bar{y})\}} \right) - \frac{c}{a + \bar{x}}\bar{y} - l_x \right) \equiv \bar{x}F(\bar{x}, \bar{y}, \bar{p}), \\ 0 &= \bar{y} \left(\hat{e} \min \left\{ 1, \frac{\bar{p}/\bar{x}}{\theta} \right\} \frac{c\bar{x}}{a + \bar{x}} - \hat{d} - l_y \right) \equiv \bar{y}G(\bar{x}, \bar{y}, \bar{p}), \\ 0 &= \frac{\hat{c}(T_P - \bar{p} - \theta \bar{y})}{\hat{a} + T_P - \bar{p} - \theta \bar{y}}\bar{x} - \frac{c\bar{p}}{a + \bar{x}}\bar{y} - d\bar{p} \equiv H(\bar{x}, \bar{y}, \bar{p}). \end{aligned}$$

Clearly the trivial extinction equilibrium $E_0 = (0, 0, 0)$ is a possible solution of this system. We can explicitly find the forms of the grazer extinction equilibria, dependent upon what is limiting the producer and other parameter-based conditions.

When the producer is phosphorus limited at equilibrium ($\bar{p}/q \leq \gamma(T_C - \bar{x})$), the grazer extinction equilibrium is given by $(\bar{x}, 0, \bar{p})$ where

$$\begin{aligned} \bar{x} &= \frac{\bar{p}}{q} \left(1 - \frac{l_x}{r} \right) = \frac{\hat{c}T_P(r - l_x)^2 - dqr(\hat{a} + T_P)(r - l_x)}{\hat{c}qr(r - l_x) - dq^2r^2}, \\ \bar{y} &= 0, \\ \bar{p} &= \frac{\hat{c}T_P(r - l_x) - dqr(\hat{a} + T_P)}{\hat{c}(r - l_x) - dqr}. \end{aligned}$$

Consider the equation for \bar{x} that includes \bar{p} . Since we require $\bar{x}, \bar{y}, \bar{p} \geq 0$ for the equilibrium to be biologically feasible, then we require $r - l_x \geq 0$, since otherwise \bar{x} is negative for positive \bar{p} . The equation for \bar{p} would also yield additional conditions for non-negativity, which are not included here.

When the producer is carbon limited at equilibrium ($\gamma(T_C - \bar{x}) \leq \bar{p}/q$), we have multiple possible grazer extinction equilibria, given by $(\bar{x}, 0, \bar{p})$ where

$$\begin{aligned} \bar{x} &= \frac{\gamma T_C(r - l_x)}{r + \gamma r - \gamma l_x}, \\ \bar{y} &= 0, \\ \bar{p} &= \frac{\hat{c}\gamma T_C(r - l_x) + d(\hat{a} + T_P)(r + \gamma r - \gamma l_x)}{2d(r + \gamma r - \gamma l_x)} \\ &\quad \pm \frac{\sqrt{(\hat{c}\gamma T_C(r - l_x) + d(\hat{a} + T_P)(r + \gamma r - \gamma l_x))^2 - 4\hat{c}d\gamma T_C T_P(r - l_x)(r + \gamma r - \gamma l_x)}}{2d(r + \gamma r - \gamma l_x)}. \end{aligned}$$

For $\bar{x} \geq 0$, we need either $r - l_x \geq 0$ and $r + \gamma r - \gamma l_x > 0$, or $r - l_x \leq 0$ and $r + \gamma r - \gamma l_x < 0$. Note that $r - l_x > 0$ and $r + \gamma r - \gamma l_x < 0$ is not possible for positive parameters. Thus, the equilibrium is not biologically feasible if $r - l_x < 0$ and $r + \gamma r - \gamma l_x > 0$. As in the phosphorus limited case, the equation for \bar{p} would also yield conditions for feasibility of the equilibria.

To determine conditions for which grazer equilibria are present dependent on parameter values, we substitute the grazer extinction equilibria found above into $\bar{p}/q = \gamma(T_C - \bar{x})$. Using the values of \bar{x} and \bar{p} for the phosphorus limited equilibrium, we require

$$\begin{aligned} \hat{c}rT_P(r - l_x) - dqr^2(\hat{a} + T_P) - \gamma T_C(\hat{c}qr(r - l_x) - dq^2r^2) \\ + \hat{c}\gamma T_P(r - l_x)^2 - dqr\gamma(\hat{a} + T_P)(r - l_x) = 0, \end{aligned}$$

for $\bar{p}/q = \gamma(T_C - \bar{x})$, and for phosphorus limited producer growth at equilibrium ($\bar{p}/q \leq \gamma(T_C - \bar{x})$), we require

$$\frac{\hat{c}rT_P(r - l_x) - dqr^2(\hat{a} + T_P) - \gamma T_C(\hat{c}qr(r - l_x) - dq^2r^2) + \hat{c}\gamma T_P(r - l_x)^2 - dqr\gamma(\hat{a} + T_P)(r - l_x)}{\hat{c}qr(r - l_x) - dq^2r^2} \leq 0.$$

Using the values of \bar{x} and \bar{p} for the carbon limited equilibrium, we require

$$\begin{aligned} 0 &= \hat{c}\gamma T_C(r - l_x) + d(\hat{a} + T_P)(r + \gamma r - \gamma l_x) - 2dqr\gamma T_C \\ &\quad \pm \sqrt{(\hat{c}\gamma T_C(r - l_x) + d(\hat{a} + T_P)(r + \gamma r - \gamma l_x))^2 - 4\hat{c}d\gamma T_C T_P(r - l_x)(r + \gamma r - \gamma l_x)} \end{aligned}$$

for $\bar{p}/q = \gamma(T_C - \bar{x})$, and for carbon limited producer growth at equilibrium ($\gamma(T_C - \bar{x}) \leq \bar{p}/q$), we require

$$\begin{aligned} 0 &\leq \frac{\hat{c}\gamma T_C(r - l_x) + d(\hat{a} + T_P)(r + \gamma r - \gamma l_x) - 2dqr\gamma T_C}{2d(r + \gamma r - \gamma l_x)} \\ &\quad \pm \frac{\sqrt{(\hat{c}\gamma T_C(r - l_x) + d(\hat{a} + T_P)(r + \gamma r - \gamma l_x))^2 - 4\hat{c}d\gamma T_C T_P(r - l_x)(r + \gamma r - \gamma l_x)}}{2d(r + \gamma r - \gamma l_x)}. \end{aligned}$$

There may also be coexistence equilibria, which would satisfy

$$0 = r \left(1 - \frac{\bar{x}}{\min\{\bar{p}/q, \gamma(T_C - \bar{x} - \bar{y})\}} \right) - \frac{c}{a + \bar{x}} \bar{y} - l_x = F(\bar{x}, \bar{y}, \bar{p}),$$

$$0 = \hat{e} \min \left\{ 1, \frac{\bar{p}/\bar{x}}{\theta} \right\} \frac{c\bar{x}}{a + \bar{x}} - \hat{d} - l_y = G(\bar{x}, \bar{y}, \bar{p}),$$

$$0 = \frac{\hat{c}(T_P - \bar{p} - \theta\bar{y})}{\hat{a} + T_P - \bar{p} - \theta\bar{y}} \bar{x} - \frac{c\bar{p}}{a + \bar{x}} \bar{y} - d\bar{p} = H(\bar{x}, \bar{y}, \bar{p}).$$

Appendix D

This appendix contains the proof of Theorem 4.

Proof Let $u = x/p$, then

$$\begin{aligned} \frac{du}{dt} &= \frac{d}{dt} \frac{x}{p} = \frac{(dx/dt)p - x(dp/dt)}{p^2} = \frac{dx/dt}{p} - x \frac{dp/dt}{p^2} \\ &= \frac{rx}{p} \left(1 - \frac{x}{\min\{p/q, h(T_C - x - y)\}} \right) - \frac{f(x)y}{p} - \frac{l_x x}{p} \\ &\quad - \frac{x^2}{p^2} g(T_P - p - \theta y) + \frac{f(x)y}{p} + d \frac{x}{p} \\ &= \frac{rx}{p} \left(1 - \frac{x}{\min\{p/q, h(T_C - x - y)\}} \right) - \frac{l_x x}{p} - \frac{x^2}{p^2} g(T_P - p - \theta y) + d \frac{x}{p} \\ &= ru \left(1 - \frac{x}{\min\{p/q, h(T_C - x - y)\}} \right) - l_x u - u^2 g(T_P - p - \theta y) + du. \end{aligned}$$

Since $g(0) = 0$ and $g'(P) > 0$ for $P \geq 0$, then $-u^2 g(T_P - p - \theta y) \leq 0$. Note that $\min\{p/q, h(T_C - x - y)\} \leq p/q$ if and only if

$$-\frac{1}{\min\{p/q, h(T_C - x - y)\}} \leq -\frac{1}{p/q}.$$

Thus

$$\begin{aligned} \frac{du}{dt} &\leq ru \left(1 - \frac{x}{p/q} \right) - l_x u + du = ru(1 - qu) - l_x u + du = ru(1 - qu) + (d - l_x)u \\ &\leq ru(1 - qu) + ru \frac{d - l_x}{r} = ru \left(1 - qu + \frac{d - l_x}{r} \right). \end{aligned}$$

Hence, $u \leq \min\{x(0)/p(0), [1 + (d - l_x)/r]/q\} \equiv m$. Consider the equation for (dp/dt) :

$$\begin{aligned} \frac{dp}{dt} &= g(T_P - p - \theta y)x - \frac{p}{x} f(x)y - dp \leq g(T_P)x - dp \leq g(T_P)mp - dp \\ &= (g(T_P)m - d)p. \end{aligned}$$

Since $d > mg(T_P)$ implies $g(T_P)m - d < 0$, then $dp/dt < 0$ and thus $p \rightarrow 0$ as $t \rightarrow \infty$.

Now, consider the equation for (dx/dt) :

$$\begin{aligned} \frac{dx}{dt} &= rx \left(1 - \frac{x}{\min\{p/q, h(T_C - x - y)\}} \right) - f(x)y - l_x x \\ &\leq rx(1 - (qx/p)). \end{aligned}$$

Hence $\limsup_{t \rightarrow \infty} x(t) \leq p/q$ and $x \rightarrow 0$ as $t \rightarrow \infty$. Given the dependence of y on x , this implies that $y \rightarrow 0$ as $t \rightarrow \infty$. Therefore, the extinction steady state $E_0 = (0, 0, 0)$ is globally asymptotically stable if $d > mg(T_P)$, where $m = \min\{x(0)/p(0), [1 + (d - l_x)/r]/q\}$. □

Appendix E

This appendix contains all the necessary calculations for the stability results in Sect. 3.3 using Holling type I functional responses for f and g .

For $f(x) = cx$, $g(P) = \hat{c}P$, and $h(C) = \gamma C$, using F, G, H as defined in ‘‘Appendix B’’,

$$\begin{aligned} \frac{\partial F}{\partial x} &= \begin{cases} -\frac{r}{p/q}, & p/q \leq \gamma(T_C - x - y), \\ -\frac{rx(T_C - y)}{\gamma(T_C - x - y)^2}, & p/q > \gamma(T_C - x - y), \end{cases} \\ \frac{\partial F}{\partial y} &= \begin{cases} -c, & p/q \leq \gamma(T_C - x - y), \\ -\frac{rx}{\gamma(T_C - x - y)^2} - c, & p/q > \gamma(T_C - x - y), \end{cases} \\ \frac{\partial F}{\partial p} &= \begin{cases} \frac{rx}{p^2/q}, & p/q \leq \gamma(T_C - x - y), \\ 0, & p/q > \gamma(T_C - x - y), \end{cases} \\ \frac{\partial G}{\partial x} &= \begin{cases} 0, & p/x \leq \theta, \\ c\hat{c}, & p/x > \theta, \end{cases} & \frac{\partial H}{\partial x} &= \hat{c}(T_P - p - \theta y), \\ \frac{\partial G}{\partial y} &= 0, & \frac{\partial H}{\partial y} &= -\hat{c}\theta x - cp, \\ \frac{\partial G}{\partial p} &= \begin{cases} \frac{c\hat{c}}{\theta}, & p/x \leq \theta, \\ 0, & p/x > \theta, \end{cases} & \frac{\partial H}{\partial p} &= -\hat{c}x - cy - d. \end{aligned}$$

We compute the products/sums we need for the Jacobian:

$$\begin{aligned} xF_x &= \begin{cases} -\frac{rx}{p/q}, & p/q \leq \gamma(T_C - x - y), \\ -\frac{rx(T_C - y)}{\gamma(T_C - x - y)^2}, & p/q > \gamma(T_C - x - y), \end{cases} \\ F + xF_x &= \begin{cases} r \left(1 - \frac{2x}{p/q} \right) - cy - l_x, & p/q \leq \gamma(T_C - x - y), \\ r \left(1 - \frac{x(2T_C - x - 2y)}{\gamma(T_C - x - y)^2} \right) - cy - l_x, & p/q > \gamma(T_C - x - y), \end{cases} \end{aligned}$$

$$\begin{aligned}
 xF_y &= \begin{cases} -cx, & p/q \leq \gamma(T_C - x - y), \\ -\frac{rx^2}{\gamma(T_C - x - y)^2} - cx, & p/q > \gamma(T_C - x - y), \end{cases} \\
 xF_p &= \begin{cases} \frac{rx^2}{p^2/q}, & p/q \leq \gamma(T_C - x - y), \\ 0, & p/q > \gamma(T_C - x - y), \end{cases} \\
 yG_x &= \begin{cases} 0, & p/x \leq \theta, \\ c\hat{e}y, & p/x > \theta, \end{cases} \\
 G + yG_y &= G = \hat{e} \min \left\{ 1, \frac{p/x}{\theta} \right\} cx - \hat{d} - l_y, \\
 yG_p &= \begin{cases} \frac{c\hat{e}y}{\theta}, & p/x \leq \theta, \\ 0, & p/x > \theta. \end{cases}
 \end{aligned}$$

Case 1 Producer nutrient limited and grazer quality limited

The corresponding Jacobian matrix with E_P from Theorem 2 substituted in is

$$A_1 = \begin{bmatrix} a_{11} & a_{12} & a_{13} \\ a_{21} & a_{22} & a_{23} \\ a_{31} & a_{32} & a_{33} \end{bmatrix},$$

where

$$\begin{aligned}
 a_{11} &= l_x - r, \\
 a_{12} &= -\frac{c\hat{c}T_P(r - l_x) - cdqr}{\hat{c}qr}, \\
 a_{13} &= \frac{(r - l_x)^2}{qr}, \\
 a_{21} &= 0, a_{22} = \frac{c\hat{c}\hat{e}T_P(r - l_x) - cd\hat{e}qr}{\hat{c}\theta(r - l_x)} - \hat{d} - l_y, \\
 a_{23} &= 0, \\
 a_{31} &= \frac{dqr}{r - l_x}, \\
 a_{32} &= -\frac{\hat{c}T_P\theta(r - l_x) - dqr\theta}{qr} - \frac{c\hat{c}T_P(r - l_x) - cdqr}{\hat{c}(r - l_x)}, \\
 a_{33} &= -\frac{\hat{c}T_P(r - l_x)}{qr}.
 \end{aligned}$$

The three eigenvalues for A_1 are (see ‘‘Appendix G’’ for proof)

$$\lambda_1 = \frac{c\hat{c}\hat{e}T_P(r - l_x) - cd\hat{e}qr}{\hat{c}\theta(r - l_x)} - \hat{d} - l_y,$$

$$\lambda_2 = -\frac{1}{2}\sqrt{\left(l_x - r + \frac{\hat{c}T_P(r - l_x)}{qr}\right)^2 + 4d(r - l_x)} + \frac{1}{2}\left(l_x - r - \frac{\hat{c}T_P(r - l_x)}{qr}\right),$$

$$\lambda_3 = \frac{1}{2}\sqrt{\left(l_x - r + \frac{\hat{c}T_P(r - l_x)}{qr}\right)^2 + 4d(r - l_x)} + \frac{1}{2}\left(l_x - r - \frac{\hat{c}T_P(r - l_x)}{qr}\right).$$

Case 2 Producer nutrient limited and grazer quantity limited

The corresponding Jacobian matrix with E_P from Theorem 2 substituted in is

$$A_2 = \begin{bmatrix} a_{11} & a_{12} & a_{13} \\ a_{21} & a_{22} & a_{23} \\ a_{31} & a_{32} & a_{33} \end{bmatrix},$$

where all entries except a_{22} are the same as in A_1 (Case 1 above), and

$$a_{22} = \frac{c\hat{c}\hat{e}T_P(r - l_x) - cd\hat{e}qr}{\hat{c}qr} - \hat{d} - l_y.$$

As in Case 1, we can explicitly find the eigenvalues for A_2 :

$$\lambda_1 = \frac{c\hat{c}\hat{e}T_P(r - l_x) - cd\hat{e}qr}{\hat{c}qr} - \hat{d} - l_y,$$

$$\lambda_2 = -\frac{1}{2}\sqrt{\left(l_x - r + \frac{\hat{c}T_P(r - l_x)}{qr}\right)^2 + 4d(r - l_x)} + \frac{1}{2}\left(l_x - r - \frac{\hat{c}T_P(r - l_x)}{qr}\right),$$

$$\lambda_3 = \frac{1}{2}\sqrt{\left(l_x - r + \frac{\hat{c}T_P(r - l_x)}{qr}\right)^2 + 4d(r - l_x)} + \frac{1}{2}\left(l_x - r - \frac{\hat{c}T_P(r - l_x)}{qr}\right).$$

Case 3 Producer carbon limited and grazer quality limited

The Jacobian with E_C from Theorem 2 substituted in takes the form

$$A_3 = \begin{bmatrix} a_{11} & a_{12} & a_{13} \\ a_{21} & a_{22} & a_{23} \\ a_{31} & a_{32} & a_{33} \end{bmatrix},$$

where

$$a_{11} = -\frac{(r - l_x)(r + \gamma r - \gamma l_x)}{r},$$

$$a_{12} = -\frac{\gamma(r - l_x)^2}{r} - \frac{c\gamma T_C(r - l_x)}{r + \gamma r - \gamma l_x}, \quad a_{13} = 0,$$

$$a_{21} = 0, \quad a_{22} = \frac{c\hat{c}\hat{e}\gamma T_C T_P(r - l_x)}{\hat{c}\gamma\theta T_C(r - l_x) + d\theta(r + \gamma r - \gamma l_x)} - \hat{d} - l_y, \quad a_{23} = 0,$$

$$a_{31} = \frac{\hat{c}dT_P(r + \gamma r - \gamma l_x)}{\hat{c}\gamma T_C(r - l_x) + d(r + \gamma r - \gamma l_x)},$$

$$a_{32} = -\frac{\hat{c}\theta\gamma T_C(r - l_x)}{r + \gamma r - \gamma l_x} - \frac{c\hat{c}\gamma T_C T_P(r - l_x)}{\hat{c}\gamma T_C(r - l_x) + d(r + \gamma r - \gamma l_x)},$$

$$a_{33} = -\frac{\hat{c}\gamma T_C(r - l_x)}{r + \gamma r - \gamma l_x} - d.$$

A 3 x 3 matrix with zeros in these specific entries has its eigenvalues along the main diagonal, since it can be decomposed into a 2 x 2 upper triangular matrix and the eigenvalue given by a_{22} . Thus, in this case

$$\lambda_1 = -\frac{(r - l_x)(r + \gamma r - \gamma l_x)}{r},$$

$$\lambda_2 = \frac{c\hat{c}\hat{e}\gamma T_C T_P(r - l_x)}{\hat{c}\gamma\theta T_C(r - l_x) + d\theta(r + \gamma r - \gamma l_x)} - \hat{d} - l_y,$$

$$\lambda_3 = -\frac{\hat{c}\gamma T_C(r - l_x)}{r + \gamma r - \gamma l_x} - d.$$

Consider $r + \gamma r - \gamma l_x$ and $r - l_x$. We see that for $r, \gamma, l_x > 0$,

$$r + \gamma r - \gamma l_x < 0 \Rightarrow r + \gamma(r - l_x) < 0 \Rightarrow r - l_x < -\frac{r}{\gamma} \Rightarrow r - l_x < 0.$$

Also, since all parameters are assumed to be positive,

$$r - l_x > 0 \Rightarrow \gamma(r - l_x) > 0 \Rightarrow r + \gamma(r - l_x) > 0 \Rightarrow r + \gamma r - \gamma l_x > 0.$$

For stability of the grazer extinction equilibrium, we need $\lambda_2 < 0$, which requires

$$\frac{c\hat{c}\hat{e}\gamma T_C T_P(r - l_x)}{\hat{c}\gamma\theta T_C(r - l_x) + d\theta(r + \gamma r - \gamma l_x)} < \hat{d} + l_y$$

and either $r + \gamma r - \gamma l_x < 0$ (in which case $r - l_x < 0$) or $r - l_x > 0$ (in which case $r + \gamma r - \gamma l_x > 0$). Then, the grazer extinction equilibrium is a stable node since $\lambda_1, \lambda_3 < 0$ when $r + \gamma r - \gamma l_x$ and $r - l_x$ have the same sign.

For either $r + \gamma r - \gamma l_x < 0$ or $r - l_x > 0$, and

$$\frac{c\hat{c}\hat{e}\gamma T_C T_P(r - l_x)}{\hat{c}\gamma\theta T_C(r - l_x) + d\theta(r + \gamma r - \gamma l_x)} > \hat{d} + l_y,$$

the grazer extinction equilibrium is a saddle with a two-dimensional stable manifold and a one-dimensional unstable manifold.

Now, for $r - l_x < 0$ and $r + \gamma r - \gamma l_x > 0$ we have a few cases. λ_1 is guaranteed to be positive, but the signs of λ_2 and λ_3 depend on additional conditions.

For $\lambda_2 < 0$, we need either $\hat{c}\gamma\theta T_C(r - l_x) + d\theta(r + \gamma r - \gamma l_x) > 0$ or $\hat{c}\gamma\theta T_C(r - l_x) + d\theta(r + \gamma r - \gamma l_x) < 0$ and

$$\frac{c\hat{c}\hat{e}\gamma T_C T_P(r - l_x)}{\hat{c}\gamma\theta T_C(r - l_x) + d\theta(r + \gamma r - \gamma l_x)} < \hat{d} + l_y.$$

For $\lambda_3 < 0$, we need

$$-\frac{\hat{c}\gamma T_C(r - l_x)}{r + \gamma r - \gamma l_x} < d.$$

Hence, for $r - l_x < 0$ and $r + \gamma r - \gamma l_x > 0$, we can have either a saddle with a one- or two-dimensional unstable manifold, or an unstable node. However, when $r - l_x < 0$ and $r + \gamma r - \gamma l_x > 0$, the equilibrium is not biologically feasible.

Case 4 Producer carbon limited and grazer quantity limited

The Jacobian with E_C from Theorem 2 substituted in is as follows:

$$A_4 = \begin{bmatrix} a_{11} & a_{12} & a_{13} \\ a_{21} & a_{22} & a_{23} \\ a_{31} & a_{32} & a_{33} \end{bmatrix},$$

where all entries are the same as A_3 (Case 3), except a_{22} and

$$a_{22} = \frac{c\hat{c}\gamma T_C(r - l_x)}{r + \gamma r - \gamma l_x} - \hat{d} - l_y.$$

As in the previous case, this matrix has its eigenvalues along the main diagonal. Thus, we have

$$\begin{aligned} \lambda_1 &= -\frac{(r - l_x)(r + \gamma r - \gamma l_x)}{r}, \\ \lambda_2 &= \frac{c\hat{c}\gamma T_C(r - l_x)}{r + \gamma r - \gamma l_x} - \hat{d} - l_y, \\ \lambda_3 &= -\frac{\hat{c}\gamma T_C(r - l_x)}{r + \gamma r - \gamma l_x} - d. \end{aligned}$$

If $r + \gamma r - \gamma l_x < 0$, then we know $r - l_x < 0$. Therefore, if $r + \gamma r - \gamma l_x < 0$, then $\lambda_1, \lambda_3 < 0$ and we also need for stability

$$\frac{c\hat{c}\gamma T_C(r - l_x)}{r + \gamma r - \gamma l_x} < \hat{d} + l_y.$$

If $r - l_x > 0$, then we know $r + \gamma r - \gamma l_x > 0$ and therefore $\lambda_1, \lambda_3 < 0$. For λ_2 to be less than 0 and therefore for stability we also require

$$\frac{c\hat{c}\gamma T_C(r - l_x)}{r + \gamma r - \gamma l_x} < \hat{d} + l_y.$$

Hence, the grazer extinction equilibrium is a stable node for

$$\frac{c\hat{e}\gamma T_C(r - l_x)}{r + \gamma r - \gamma l_x} < \hat{d} + l_y$$

and either $r + \gamma r - \gamma l_x < 0$ or $r - l_x > 0$.

For either $r + \gamma r - \gamma l_x < 0$ or $r - l_x > 0$, and

$$\frac{c\hat{e}\gamma T_C(r - l_x)}{r + \gamma r - \gamma l_x} > \hat{d} + l_y,$$

the grazer extinction equilibrium is a saddle with a two-dimensional stable manifold and a one-dimensional unstable manifold.

For $r - l_x < 0$ and $r + \gamma r - \gamma l_x > 0$, we have $\lambda_1 > 0$ and $\lambda_2 < 0$. Therefore, we have a saddle. If $\lambda_3 < 0$, the saddle has a two-dimensional stable manifold and a one-dimensional unstable manifold; if $\lambda_3 > 0$, it has a one-dimensional stable manifold and a two-dimensional unstable manifold. Note that for $r - l_x < 0$ and $r + \gamma r - \gamma l_x > 0$, the equilibrium is not biologically feasible.

Appendix F

This appendix contains all the necessary calculations for the stability results in Sect. 3.3 using Holling type II functional responses for f and g .

For $f(x) = cx/(a + x)$, $g(P) = \hat{c}P/(\hat{a} + P)$, and $h(C) = \gamma C$, using F, G, H as defined in ‘‘Appendix C’’,

$$\begin{aligned} \frac{\partial F}{\partial x} &= \begin{cases} -\frac{r}{p/q} + \frac{cy}{(a+x)^2}, & p/q \leq \gamma(T_C - x - y), \\ -\frac{r(T_C - y)}{\gamma(T_C - x - y)^2} + \frac{cy}{(a+x)^2}, & p/q > \gamma(T_C - x - y), \end{cases} \\ \frac{\partial F}{\partial y} &= \begin{cases} -\frac{c}{a+x}, & p/q \leq \gamma(T_C - x - y), \\ -\frac{rx}{\gamma(T_C - x - y)^2} - \frac{c}{a+x}, & p/q > \gamma(T_C - x - y), \end{cases} \\ \frac{\partial F}{\partial p} &= \begin{cases} \frac{rx}{p^2/q}, & p/q \leq \gamma(T_C - x - y), \\ 0, & p/q > \gamma(T_C - x - y), \end{cases} \\ \frac{\partial G}{\partial x} &= \begin{cases} -\frac{\hat{c}\hat{e}p}{\theta(a+x)^2}, & p/x \leq \theta, \\ \frac{ac\hat{e}}{(a+x)^2}, & p/x > \theta, \end{cases} \\ \frac{\partial G}{\partial y} &= 0, \\ \frac{\partial G}{\partial p} &= \begin{cases} \frac{\hat{c}\hat{e}}{\theta(a+x)}, & p/x \leq \theta, \\ 0, & p/x > \theta, \end{cases} \\ \frac{\partial H}{\partial x} &= \frac{\hat{c}(T_P - p - \theta y)}{\hat{a} + T_P - p - \theta y} + \frac{cpy}{(a + x)^2}, \end{aligned}$$

$$\frac{\partial H}{\partial y} = -\frac{\hat{a}\hat{c}\theta x}{(\hat{a} + T_P - p - \theta y)^2} - \frac{cp}{a + x},$$

$$\frac{\partial H}{\partial p} = -\frac{\hat{a}\hat{c}x}{(\hat{a} + T_P - p - \theta y)^2} - \frac{cy}{a + x} - d.$$

The necessary products and sums for the Jacobian are

$$xF_x = \begin{cases} -\frac{rx}{p/q} + \frac{cxy}{(a+x)^2}, & p/q \leq \gamma(T_C - x - y), \\ -\frac{rx(T_C - y)}{\gamma(T_C - x - y)^2} + \frac{cxy}{(a+x)^2}, & p/q > \gamma(T_C - x - y), \end{cases}$$

$$F + xF_x = \begin{cases} r\left(1 - \frac{2x}{p/q}\right) - \frac{acy}{(a+x)^2} - l_x, & p/q \leq \gamma(T_C - x - y), \\ r\left(1 - \frac{x(2T_C - x - 2y)}{\gamma(T_C - x - y)^2}\right) - \frac{acy}{(a+x)^2} - l_x, & p/q > \gamma(T_C - x - y), \end{cases}$$

$$xF_y = \begin{cases} -\frac{cx}{a+x}, & p/q \leq \gamma(T_C - x - y), \\ -\frac{rx^2}{\gamma(T_C - x - y)^2} - \frac{cx}{a+x}, & p/q > \gamma(T_C - x - y), \end{cases}$$

$$xF_p = \begin{cases} \frac{rx^2}{p^2/q}, & p/q \leq \gamma(T_C - x - y), \\ 0, & p/q > \gamma(T_C - x - y), \end{cases}$$

$$yG_x = \begin{cases} -\frac{c\hat{e}py}{\theta(a+x)^2}, & p/x \leq \theta, \\ \frac{ac\hat{e}y}{(a+x)^2}, & p/x > \theta, \end{cases}$$

$$G + yG_y = G = \hat{e}\min\left\{1, \frac{p/x}{\theta}\right\} \frac{cx}{a+x} - \hat{d} - l_y,$$

$$yG_p = \begin{cases} \frac{c\hat{e}y}{\theta(a+x)}, & p/x \leq \theta, \\ 0, & p/x > \theta. \end{cases}$$

Case 1 Producer nutrient limited and grazer quality limited

The corresponding Jacobian matrix with E_P from Theorem 3 substituted in is

$$B_1 = \begin{bmatrix} b_{11} & b_{12} & b_{13} \\ b_{21} & b_{22} & b_{23} \\ b_{31} & b_{32} & b_{33} \end{bmatrix},$$

where for $E_P = (\bar{x}, 0, \bar{p})$ (Theorem 3)

$$b_{11} = l_x - r,$$

$$b_{12} = -\frac{c\bar{p}(r - l_x)}{arq + \bar{p}(r - l_x)},$$

$$b_{13} = \frac{(r - l_x)^2}{qr},$$

$$\begin{aligned}
 b_{21} &= 0, \\
 b_{22} &= \frac{c\hat{c}qr\bar{p}}{\theta(aqr + \bar{p}(r - l_x))} - \hat{d} - l_y, \\
 b_{23} &= 0, \\
 b_{31} &= \frac{dqr}{r - l_x} \\
 b_{32} &= -\frac{\hat{a}\hat{c}\theta\bar{p}(r - l_x)}{qr(\hat{a} + T_P - \bar{p})^2} - \frac{cqr\bar{p}}{aqr + \bar{p}(r - l_x)}, \\
 b_{33} &= -\frac{\hat{a}\hat{c}\bar{p}(r - l_x)}{qr(\hat{a} + T_P - \bar{p})^2} - d.
 \end{aligned}$$

As in Holling type I Case 1, we can explicitly determine the eigenvalues:

$$\begin{aligned}
 \lambda_1 &= \frac{c\hat{c}qr\bar{p}}{\theta(aqr + \bar{p}(r - l_x))} - \hat{d} - l_y, \\
 \lambda_2 &= -\frac{1}{2}\sqrt{\left(l_x - r + \frac{\hat{a}\hat{c}\bar{p}(r - l_x)}{qr(\hat{a} + T_P - \bar{p})^2} + d\right)^2 + 4d(r - l_x)} \\
 &\quad + \frac{1}{2}\left(l_x - r - \frac{\hat{a}\hat{c}\bar{p}(r - l_x)}{qr(\hat{a} + T_P - \bar{p})^2} - d\right), \\
 \lambda_3 &= \frac{1}{2}\sqrt{\left(l_x - r + \frac{\hat{a}\hat{c}\bar{p}(r - l_x)}{qr(\hat{a} + T_P - \bar{p})^2} + d\right)^2 + 4d(r - l_x)} \\
 &\quad + \frac{1}{2}\left(l_x - r - \frac{\hat{a}\hat{c}\bar{p}(r - l_x)}{qr(\hat{a} + T_P - \bar{p})^2} - d\right).
 \end{aligned}$$

Again, the eigenvalues are not particularly illuminating. Also similar to the Holling type I case, stability does not depend on T_C or γ . Given the producer is nutrient limited at this equilibrium, it is reasonable that the carbon-dependent carrying capacity has no impact on its stability.

Case 2 Producer nutrient limited and grazer quantity limited

The corresponding Jacobian with E_P from Theorem 3 substituted in is

$$B_2 = \begin{bmatrix} b_{11} & b_{12} & b_{13} \\ b_{21} & b_{22} & b_{23} \\ b_{31} & b_{32} & b_{33} \end{bmatrix},$$

where all entries are the same as B_1 (Case 1) except b_{22} , which is

$$b_{22} = \frac{c\hat{c}\bar{p}(r - l_x)}{aqr + \bar{p}(r - l_x)} - \hat{d} - l_y,$$

for $E_P = (\bar{x}, 0, \bar{p})$ (Theorem 3).

The eigenvalues are

$$\begin{aligned} \lambda_1 &= \frac{c\hat{e}\bar{p}(r - l_x)}{aqr + \bar{p}(r - l_x)} - \hat{d} - l_y, \\ \lambda_2 &= -\frac{1}{2}\sqrt{\left(l_x - r + \frac{\hat{a}\hat{c}\bar{p}(r - l_x)}{qr(\hat{a} + T_P - \bar{p})^2} + d\right)^2 + 4d(r - l_x)} \\ &\quad + \frac{1}{2}\left(l_x - r - \frac{\hat{a}\hat{c}\bar{p}(r - l_x)}{qr(\hat{a} + T_P - \bar{p})^2} - d\right), \\ \lambda_3 &= \frac{1}{2}\sqrt{\left(l_x - r + \frac{\hat{a}\hat{c}\bar{p}(r - l_x)}{qr(\hat{a} + T_P - \bar{p})^2} + d\right)^2 + 4d(r - l_x)} \\ &\quad + \frac{1}{2}\left(l_x - r - \frac{\hat{a}\hat{c}\bar{p}(r - l_x)}{qr(\hat{a} + T_P - \bar{p})^2} - d\right). \end{aligned}$$

The eigenvalues do not provide any stability conclusions in this case. As in Case 2 for Holling type I functional responses, stability does not depend on T_C , γ , or θ . The producer is nutrient limited at equilibrium, so T_C and γ should not impact stability of the equilibrium. Note that since the grazer is quantity limited at equilibrium, we would also expect the stability of the equilibrium to not depend on the grazer’s P:C ratio, θ .

Case 3 Producer carbon limited and grazer quality limited

Here we use E_{C+} or E_{C-} from Theorem 3 and compute

$$B_3 = \begin{bmatrix} b_{11} & b_{12} & b_{13} \\ b_{21} & b_{22} & b_{23} \\ b_{31} & b_{32} & b_{33} \end{bmatrix},$$

where

$$\begin{aligned} b_{11} &= -\frac{(r - l_x)(r + \gamma r - \gamma l_x)}{r}, \\ b_{12} &= -\frac{\gamma(r - l_x)^2}{r} - \frac{c\gamma T_C(r - l_x)}{a(r + \gamma r - \gamma l_x) + \gamma T_C(r - l_x)}, \\ b_{13} &= 0, \\ b_{21} &= 0, \\ b_{22} &= \frac{c\hat{e}(r + \gamma r - \gamma l_x)\bar{p}}{a\theta(r + \gamma r - \gamma l_x) + \gamma\theta T_C(r - l_x)} - \hat{d} - l_y, \\ b_{23} &= 0, \\ b_{31} &= \frac{\hat{c}(T_P - \bar{p})}{\hat{a} + T_P - \bar{p}}, \\ b_{32} &= -\frac{\hat{a}\hat{c}\gamma\theta T_C(r - l_x)}{(r + \gamma r - \gamma l_x)(\hat{a} + T_P - \bar{p})^2} - \frac{c(r + \gamma r - \gamma l_x)\bar{p}}{a(r + \gamma r - \gamma l_x) + \gamma T_C(r - l_x)}, \end{aligned}$$

$$b_{33} = -\frac{\hat{a}\hat{c}\gamma T_C(r - l_x)}{(r + \gamma r - \gamma l_x)(\hat{a} + T_P - \bar{p})^2} - d,$$

where \bar{x} and \bar{p} correspond to the possible carbon-limited equilibrium values from Theorem 3.

The corresponding eigenvalues are along the main diagonal, as in the corresponding Holling type I case:

$$\begin{aligned} \lambda_1 &= -\frac{(r - l_x)(r + \gamma r - \gamma l_x)}{r}, \\ \lambda_2 &= \frac{c\hat{c}(r + \gamma r - \gamma l_x)\bar{p}}{a\theta(r + \gamma r - \gamma l_x) + \gamma\theta T_C(r - l_x)} - \hat{d} - l_y, \\ \lambda_3 &= -\frac{\hat{a}\hat{c}\gamma T_C(r - l_x)}{(r + \gamma r - \gamma l_x)(\hat{a} + T_P - \bar{p})^2} - d. \end{aligned}$$

For these eigenvalues, we consider stability cases using $r - l_x$ and $r + \gamma r - \gamma l_x$. As in the Holling type I case, we recognize that $r + \gamma r - \gamma l_x < 0$ implies $r - l_x < 0$, and $r - l_x > 0$ implies $r + \gamma r - \gamma l_x > 0$, when all parameters are assumed to be positive. Therefore we consider three cases.

If $r + \gamma r - \gamma l_x < 0$ (and therefore $r - l_x < 0$), then $\lambda_1 < 0$ and $\lambda_3 < 0$. The sign of λ_2 depends on the sign of \bar{p} . Looking at the forms of the equilibria in Sect. 3.2, we observe that for $r + \gamma r - \gamma l_x < 0$ and $r - l_x < 0$, both equilibria have a positive \bar{p} . Hence, the equilibrium is a stable node for $r + \gamma r - \gamma l_x < 0$ and

$$\frac{c\hat{c}(r + \gamma r - \gamma l_x)\bar{p}}{a\theta(r + \gamma r - \gamma l_x) + \gamma\theta T_C(r - l_x)} < \hat{d} + l_y.$$

If $r + \gamma r - \gamma l_x < 0$ but the additional condition is not satisfied, then the equilibrium is a saddle with a two-dimensional stable manifold and a one-dimensional unstable manifold.

If $r - l_x > 0$ (and therefore $r + \gamma r - \gamma l_x > 0$), then $\lambda_1 < 0$ and $\lambda_3 < 0$. Since $\bar{p} > 0$ for $r - l_x > 0$ and both forms of \bar{p} , then the equilibrium is a stable node for $r - l_x > 0$ and

$$\frac{c\hat{c}(r + \gamma r - \gamma l_x)\bar{p}}{a\theta(r + \gamma r - \gamma l_x) + \gamma\theta T_C(r - l_x)} < \hat{d} + l_y.$$

If $r - l_x > 0$ but $\lambda_2 > 0$ because the above condition is not satisfied, then the equilibrium is a saddle with a two-dimensional stable manifold and a one-dimensional unstable manifold.

Lastly, if $r - l_x < 0$ and $r + \gamma r - \gamma l_x > 0$, then $\lambda_1 > 0$. The signs of λ_2 and λ_3 depend on additional conditions. For the equilibrium to be a saddle with a two-dimensional stable manifold and a one-dimensional unstable manifold when $r - l_x < 0$ and $r + \gamma r - \gamma l_x > 0$, we require

$$\frac{c\hat{c}(r + \gamma r - \gamma l_x)\bar{p}}{a\theta(r + \gamma r - \gamma l_x) + \gamma\theta T_C(r - l_x)} < \hat{d} + l_y,$$

$$-\frac{\hat{a}\hat{c}\gamma T_C(r - l_x)}{(r + \gamma r - \gamma l_x)(\hat{a} + T_P - \bar{p})^2} < d.$$

Note that here the sign of \bar{p} is not determined by the signs of $r - l_x$ and $r + \gamma r - \gamma l_x$ alone. If either one of these additional conditions is not satisfied (i.e., $\lambda_2 > 0$ or $\lambda_3 > 0$) and the other is satisfied, then the equilibrium is a saddle with a one-dimensional stable manifold and a two-dimensional unstable manifold. If both of these additional conditions are not satisfied, then the equilibrium is an unstable node. However, in this case, the equilibrium is only biologically feasible when the signs of $r - l_x$ and $r + \gamma r - \gamma l_x$ are the same.

Case 4 Producer carbon limited and grazer quantity limited

The Jacobian with E_{C+} or E_{C-} from Theorem 3 substituted in takes the form

$$B_4 = \begin{bmatrix} b_{11} & b_{12} & b_{13} \\ b_{21} & b_{22} & b_{23} \\ b_{31} & b_{32} & b_{33} \end{bmatrix},$$

where all entries are the same as in B_3 , except

$$b_{22} = \frac{c\hat{c}\gamma T_C(r - l_x)}{a(r + \gamma r - \gamma l_x) + \gamma T_C(r - l_x)} - \hat{d} - l_y.$$

Once again, the eigenvalues are along the main diagonal, using \bar{p} from E_{C+} or E_{C-} from Theorem 3:

$$\begin{aligned} \lambda_1 &= -\frac{(r - l_x)(r + \gamma r - \gamma l_x)}{r}, \\ \lambda_2 &= \frac{c\hat{c}\gamma T_C(r - l_x)}{a(r + \gamma r - \gamma l_x) + \gamma T_C(r - l_x)} - \hat{d} - l_y, \\ \lambda_3 &= -\frac{\hat{a}\hat{c}\gamma T_C(r - l_x)}{(r + \gamma r - \gamma l_x)(\hat{a} + T_P - \bar{p})^2} - d. \end{aligned}$$

We consider cases based on $r - l_x$ and $r + \gamma r - \gamma l_x$. Note that we cannot have $r - l_x > 0$ and $r + \gamma r - \gamma l_x < 0$ for positive r, γ and l_x .

If $r - l_x < 0$ and $r + \gamma r - \gamma l_x < 0$, then $\lambda_1 < 0$ and $\lambda_3 < 0$. Therefore, the equilibrium is a stable node if $r + \gamma r - \gamma l_x < 0$ and

$$\frac{c\hat{c}\gamma T_C(r - l_x)}{a(r + \gamma r - \gamma l_x) + \gamma T_C(r - l_x)} < \hat{d} + l_y.$$

If this additional condition is not satisfied (i.e., $\lambda_2 > 0$), then the equilibrium is a saddle with a two-dimensional stable manifold and a one-dimensional unstable manifold.

Similarly, if $r - l_x > 0$ and $r + \gamma r - \gamma l_x > 0$, then $\lambda_1 < 0$ and $\lambda_3 < 0$. Hence, the equilibrium is a stable node if $r - l_x > 0$ and

$$\frac{c\hat{c}\gamma T_C(r - l_x)}{a(r + \gamma r - \gamma l_x) + \gamma T_C(r - l_x)} < \hat{d} + l_y.$$

If the above condition is not satisfied, then the equilibrium is a saddle with a two-dimensional stable manifold and a one-dimensional unstable manifold.

If $r - l_x < 0$ and $r + \gamma r - \gamma l_x > 0$, then $\lambda_1 > 0$. The equilibrium is a saddle with a two-dimensional stable manifold and a one-dimensional unstable manifold if

$$\frac{c\hat{e}\gamma T_C(r - l_x)}{a(r + \gamma r - \gamma l_x) + \gamma T_C(r - l_x)} < \hat{d} + l_y,$$

$$-\frac{\hat{a}\hat{c}\gamma T_C(r - l_x)}{(r + \gamma r - \gamma l_x)(\hat{a} + T_P - \bar{p})^2} < d.$$

If either of these conditions is not met, the equilibrium is a saddle with a one-dimensional stable manifold and a two-dimensional unstable manifold; if both conditions are not met, the equilibrium is an unstable node. Note that if $r - l_x < 0$ and $r + \gamma r - \gamma l_x > 0$, then the equilibrium is not biologically feasible.

Appendix G

This appendix proves the form of the eigenvalues for the nutrient limited grazer extinction equilibria.

Claim: For a matrix of the form

$$A = \begin{bmatrix} a & b & c \\ 0 & d & 0 \\ f & g & h \end{bmatrix}$$

where all entries are real numbers, the eigenvalues are

$$\lambda_1 = d,$$

$$\lambda_2 = \frac{1}{2} \left(-\sqrt{(a - h)^2 + 4cf} + a + h \right),$$

$$\lambda_3 = \frac{1}{2} \left(\sqrt{(a - h)^2 + 4cf} + a + h \right).$$

Proof We know an eigenvalue λ of matrix A satisfies $\det(A - \lambda I) = 0$. Hence, we solve this equation for λ .

We see that

$$\det(A - \lambda I) = \det \left(\begin{bmatrix} a - \lambda & b & c \\ 0 & d - \lambda & 0 \\ f & g & h - \lambda \end{bmatrix} \right).$$

Using a cofactor expansion along the second row, we see

$$\det(A - \lambda I) = (d - \lambda)\det \left(\begin{bmatrix} a - \lambda & c \\ f & h - \lambda \end{bmatrix} \right)$$

$$\begin{aligned}
 &= (d - \lambda)((a - \lambda)(h - \lambda) - cf) \\
 &= (d - \lambda)(ah - (a + h)\lambda + \lambda^2 - cf) \\
 &= (d - \lambda)(\lambda^2 - (a + h)\lambda + (ah - cf)).
 \end{aligned}$$

We can find solutions to the following using the quadratic formula:

$$(d - \lambda)(\lambda^2 - (a + h)\lambda + (ah - cf)) = 0.$$

The resulting solutions are

$$\begin{aligned}
 \lambda_1 &= d, \\
 \lambda_2 &= \frac{1}{2} \left(\sqrt{(a + h)^2 - 4(ah - cf)} + a + h \right), \\
 \lambda_3 &= \frac{1}{2} \left(-\sqrt{(a + h)^2 - 4(ah - cf)} + a + h \right).
 \end{aligned}$$

Clearly

$$\begin{aligned}
 (a + h)^2 - 4(ah - cf) &= a^2 + 2ah + h^2 - 4ah + 4cf \\
 &= a^2 - 2ah + h^2 + 4cf = (a - h)^2 + 4cf,
 \end{aligned}$$

and this proves the claim. \square

References

- Ainsworth EA, Rogers A (2007) The response of photosynthesis and stomatal conductance to rising $[\text{CO}_2]$: mechanisms and environmental interactions. *Plant Cell Environ* 30(3):258–270. <https://doi.org/10.1111/j.1365-3040.2007.01641.x>
- Burkhardt S, Riebesell U (1997) CO_2 availability affects elemental composition (C:N:P) of the marine diatom *Skeletonema costatum*. *Mar Ecol Prog Ser* 155:67–76. <https://doi.org/10.3354/meps155067>
- Davies CM, Wang H (2020) Contrasting stoichiometric dynamics in terrestrial and aquatic grazer–producer systems. *J Biol Dyn*. <https://doi.org/10.1080/17513758.2020.1771442>
- de Graaff MA, van Groenigen KJ, Six J, Hungate B, van Kessel C (2006) Interactions between plant growth and soil nutrient cycling under elevated CO_2 : a meta-analysis. *Glob Change Biol* 12(11):2077–2091. <https://doi.org/10.1111/j.1365-2486.2006.01240.x>
- De Kauwe MG, Medlyn BE, Zaehle S et al (2013) Forest water use and water use efficiency at elevated CO_2 : a model-data intercomparison at two contrasting temperate forest FACE sites. *Glob Change Biol* 19(6):1759–1779. <https://doi.org/10.1111/gcb.12164>
- Dhooge A, Govaerts W, Kuznetsov YA, Meijer HGE, Sautois B (2008) New features of the software MatCont for bifurcation analysis of dynamical systems. *Math Comput Model Dyn Syst* 14(2):147–175. <https://doi.org/10.1080/13873950701742754>
- Diehl S (2007) Paradoxes of enrichment: effects of increased light versus nutrient supply on pelagic producer–grazer systems. *Am Nat* 169(6):E173–E191. <https://doi.org/10.1086/516655>
- Drake BG, González-Meler MA, Long SP (1997) More efficient plants: A consequence of rising atmospheric CO_2 ? *Annu Rev Plant Biol* 48(1):609–639. <https://doi.org/10.1146/annurev.arplant.48.1.609>
- Du C, Wang X, Zhang M, Jing J, Gao Y (2019) Effects of elevated CO_2 on plant CNP stoichiometry in terrestrial ecosystems: a meta-analysis. *Sci Total Environ* 650:697–708. <https://doi.org/10.1016/j.scitotenv.2018.09.051>

- Elser JJ, Fagan WF, Kerkhoff AJ, Swenson NG, Enquist BJ (2010) Biological stoichiometry of plant production: metabolism, scaling and ecological response to global change. *New Phytol* 186(3):593–608. <https://doi.org/10.1111/j.1469-8137.2010.03214.x>
- Hessen DO, Elser JJ, Sterner RW, Urabe J (2013) Ecological stoichiometry: an elementary approach using basic principles. *Limnol Oceanogr* 58(6):2219–2236. <https://doi.org/10.4319/lo.2013.58.6.2219>
- Körner C (2009) Responses of humid tropical trees to rising CO₂. *Annu Rev Ecol Evol Syst* 40:61–79. <https://doi.org/10.1146/annurev.ecolsys.110308.120217>
- Leakey ADB, Ainsworth EA, Bernacchi CJ, Rogers A, Long SP, Ort DR (2009) Elevated CO₂ effects on plant carbon, nitrogen, and water relations: six important lessons from FACE. *J Exp Bot* 60(10):2859–2876. <https://doi.org/10.1093/jxb/erp096>
- Loladze I, Kuang Y, Elser JJ (2000) Stoichiometry in producer–grazer systems: linking energy flow with element cycling. *Bull Math Biol* 62(6):1137–1162. <https://doi.org/10.1006/bulm.2000.0201>
- Long SP, Drake BG (1991) Effect of the long-term elevation of CO₂ concentration in the field on the quantum yield of photosynthesis of the C₃ sedge, *Scirpus olneyi*. *Plant Physiol* 96(1):221–226. <https://doi.org/10.1104/pp.96.1.221>
- Lovelock CE, Kyllö D, Winter K (1996) Growth responses to vesicular-arbuscular mycorrhizae and elevated CO₂ in seedlings of a tropical tree, *Beilschmiedia pendula*. *Funct Ecol*. <https://doi.org/10.2307/2390177>
- Low-Decarie E, Fussmann GF, Bell G (2014) Aquatic primary production in a high-CO₂ world. *Trends Ecol Evol* 29(4):223–232. <https://doi.org/10.1016/j.tree.2014.02.006>
- Pachauri RK, Allen MR, Barros VR et al (2014) Climate change 2014: synthesis report. In: Contribution of Working Groups I, II and III to the fifth assessment report of the Intergovernmental Panel on Climate Change. IPCC
- Petrucci RH, Herring FG, Madura JD, Bissonnette C (2011) General chemistry: principles and modern applications, 10th edn. Pearson Canada Inc
- Pugh TAM, Müller C, Arneith A, Haverd V, Smith B (2016) Key knowledge and data gaps in modelling the influence of CO₂ concentration on the terrestrial carbon sink. *J Plant Physiol* 203:3–15. <https://doi.org/10.1016/j.jplph.2016.05.001>
- Spijkerman E, de Castro F, Gaedke U (2011) Independent colimitation for carbon dioxide and inorganic phosphorus. *PLoS One*. <https://doi.org/10.1371/journal.pone.0028219>
- Sterner RW, Elser JJ (2002) Ecological stoichiometry: the biology of elements from molecules to the biosphere. Princeton University Press
- Stitt M, Lunn J, Usadel B (2010) Arabidopsis and primary photosynthetic metabolism—more than the icing on the cake. *Plant J* 61(6):1067–1091. <https://doi.org/10.1111/j.1365-313X.2010.04142.x>
- Urabe J, Togari J, Elser JJ (2003) Stoichiometric impacts of increased carbon dioxide on a planktonic herbivore. *Glob Change Biol* 9(6):818–825. <https://doi.org/10.1046/j.1365-2486.2003.00634.x>
- van de Waal DB, Verschoor AM, Verspagen JM et al (2010) Climate-driven changes in the ecological stoichiometry of aquatic ecosystems. *Front Ecol Environ* 8(3):145–152. <https://doi.org/10.1890/080178>
- von Caemmerer S, Quick WP (2000) Rubisco: physiology in vivo. In: Leegood RC, Sharkey TD, von Caemmerer S (eds) Photosynthesis. Springer, Dordrecht, pp 85–113
- Wang H, Kuang Y, Loladze I (2008) Dynamics of a mechanistically derived stoichiometric producer–grazer model. *J Biol Dyn* 2(3):286–296. <https://doi.org/10.1080/17513750701769881>
- Wanninkhof R (2007) The impact of different gas exchange formulations and wind speed products on global air–sea CO₂ fluxes. In: Garbe CS, Handler RA, Jähne B (eds) Transport at the air–sea interface. Springer, Berlin, pp 1–23
- Würth MKR, Winter K, Körner C (1998) In situ responses to elevated CO₂ in tropical forest understorey plants. *Funct Ecol* 12(6):886–895. <https://doi.org/10.1046/j.1365-2435.1998.00278.x>

Publisher's Note Springer Nature remains neutral with regard to jurisdictional claims in published maps and institutional affiliations.